IEEE Access
Multidisciplinary | Rapid Review | Open Access Journal

Received 17 January 2024, accepted 17 February 2024, date of publication 20 February 2024, date of current version 5 March 2024.

Digital Object Identifier 10.1109/ACCESS.2024.3367828

RESEARCH ARTICLE

Real-Time Validation of Intelligent Super-Twisting Sliding Mode Control for Variable-Speed DFIG Using dSPACE 1104 Board

MOURAD YESSEF[1], HABIB BENBOUHENNI[2], MOHAMMED TAOUSSI[3], AHMED LAGRIOUI[4], ILHAMI COLAK[2], SALEH MOBAYEN[5], (Senior Member, IEEE), ANTON ZHILENKOV[6], (Senior Member, IEEE), AND BADRE BOSSOUFI[1]

[1]LIMAS Laboratory, Faculty of Sciences Dhar El Mahraz, Sidi Mohamed Ben Abdellah (SMBA) University, Fes 30000, Morocco
[2]Department of Electrical and Electronics Engineering, Faculty of Engineering and Architecture, Nişantaşi University, 34481742 Istanbul, Turkey
[3]Higher School of Technology, SMBA University, Fes 30000, Morocco
[4]ENSAM, Moulay Ismail University, Meknes 50000, Morocco
[5]Graduate School of Intelligent Data Science, National Yunlin University of Science and Technology, Douliou, Yunlin 640301, Taiwan
[6]Department of Cyber-Physical Systems, Saint Petersburg State Marine Technical University, 190121 Saint-Petersburg, Russia

Corresponding authors: Mourad Yessef (mourad.yessef@usmba.ac.ma) and Saleh Mobayen (mobayens@yuntech.edu.tw)

ABSTRACT The super-twisting sliding mode controller (STSMC) is considered one of the simplest and easiest to implement nonlinear controls, as it can be easily applied in industrial systems. Using this controller leads to reducing the phenomenon of chatter and significantly increasing the durability of the systems. However, this controller has several drawbacks and problems, as its use does not lead to improving the systems as required. In this study, an idea has been proposed based on the use of neural networks in order to overcome the defects and problems of the STSMC strategy. This proposed strategy is used to increase the durability and improve the characteristics of an energy system based on wind turbines using a dual induction generator. The latter is controlled by direct power control (DPC). The proposed controller was used to control energies, where the pulse width modulation strategy was used to convert voltage reference values into pulses to operate the rotor side converter. Therefore, simplicity, durability, outstanding performance, ease of implementation, few gains, and low cost are among the most prominent features of the proposed intelligent STSMC technique and control. The MATLAB environment was used first to implement the proposed energy system under different working conditions using variable wind speed, where the proposed controller was compared with the performance of the STSMC technique. The proposed intelligent STSMC technique was implemented experimentally using the dSPACE 1104 Card to verify the performance and the validity of the simulated results. The experimental results show the effectiveness and ability of the proposed controller to improve the characteristics of the DPC strategy and the energy system as a whole.

INDEX TERMS Neural algorithms, super-twisting-direct power command, dSPACE 1104 Card, doubly-feed induction generator.

NOMENCLATURE

DPC	Direct power control.
STSMC	Super-twisting sliding mode controller.
DFIG	Doubly-fed induction generator.
PWM	Pulse width modulation.
MPPT	Maximum power point tracking.
REs	Renewable energies.
ST	Switching table.
HC	Hysteresis comparator.

The associate editor coordinating the review of this manuscript and approving it for publication was Hongli Dong.

WEG	Wind energy conversion.
WTS	Wind turbine system.
DTC	Direct torque control.
THD	Total harmonic distortion.
FOC	Field-oriented control.
RSC	Rotor side converter.
SMC	Sliding mode controller.
BC	Backstepping control.
VSWT	Variable-speed wind turbines.
Ps	Active power.
GSC	Grid side converter.
Qs	Reactive power.
DVC	Direct vector control.
PMSMs	Permanent magnet synchronous machines.
ANN	Artificial neural network.
EP	Electrical power.
IVC	Indirect vector control.
SVM	Space vector modulation.
PI	Proportional-integral controller.
SC	Synergetic command.
NSTSMC	Neural super-twisting sliding mode controller.
WS	Wind speed.

I. INTRODUCTION

Electric power (EP) is among the powers of the universe that changed human life for the better. It is crucial in the economy and growth, as it is among the basics of economic excellence. EP is obtained by converting other energies, such as mechanical energy, using electrical machines for this purpose, as the cost of producing and consuming EP is largely related to the generation systems. These systems are as diverse as the EP production sources. To generate EP, traditional sources, renewable sources, and hybrid sources can be used. Depending on the type of source used, the EP generating station is named. Using traditional sources such as coal for energy generation leads to undesirable results such as the emission of toxic gases [1]. The latter affects the environment and human life, prompting governments and researchers to search for more appropriate and effective solutions to protecting the environment from pollution and reducing the utilization of traditional energy sources and the costs of producing EPs. Also, the use of traditional sources in the production of EP does not lead to a reduction in the EP consumption bill, which is a negative matter that increases the burden on the level of private individuals and companies, allowing for higher costs for other manufactured materials.

In recent years, the idea of renewable energies (REs) has come to light as a suitable solution for generating EP and protecting the environment from gas emissions risks. Especially after the Tokyo Treaty of 1997, governments pledged to reduce the use of traditional sources in generating EP and resort to clean sources that do not release toxic gases, in order to overcome the phenomenon of global warming that has begun to affect several countries around the world [2]. These RE sources are diverse: wind energy (WE), water energy, sun energy, wave energy, ocean current energy,...etc. These sources are available in nature all year round and are characterized by being free and easy to exploit compared to traditional sources. In addition, the use of these sources does not contribute to the release of toxic gases, and thus the severity of the global warming phenomenon is reduced [3]. Exploiting these sources in the production of EP leads to reducing the costs of production, transportation, and distribution of energy, which also contributes to reducing the energy consumption bill, which encourages economic growth in poor countries [4].

One of the most prominent REs that has proven its importance in generating EP is the WE. The use of this energy source is uncomplicated and does not require complex technology, which allows for cost reductions [5]. This energy source is considered clean energy and is available all year round. To exploit this energy source, turbines called wind turbines are used [6]. These turbines are used in the form of farms called wind farms. The latter is accomplished on land and at sea. Wind turbines convert WE into mechanical energy, where the gained energy is later converted into EP. This energy gain is related to the size of the turbine, as the larger the dimensions of the turbine, the greater the energy gained [7]. Also, the speed and shape of the wind have an effect on the energy gained, as the higher the WS, the greater the value of the energy gained, and vice versa. In these turbines, blades are used to obtain mechanical energy from the wind [8]. One, two, and three blades are used. Three-blade turbines are the most widely used turbines in the field of wind energy [9].

In the industry, there are two kinds of wind power generators (WEGs): Variable-speed wind turbines (VSWTs) and fixed-speed wind turbines [10]. However, the first kind ensures wide-range operations regarding improved efficiency, higher energy-capturing capabilities, and wind speed (WS). Therefore, the efficiency of VSWTs exceeds that of fixed-speed wind turbines [11]. Also, in terms of cost, complexity, control, and maintenance, VSWTs are superior to other types. The use of wind turbines has several disadvantages and problems. They cannot withstand strong winds (especially hurricanes) and fires, and therefore they are quickly destroyed, and fires cannot be extinguished at their level, which increases industrial costs [12]. Also, the turbines should not be placed in the path of migrating birds, and the lifespan of the energy system is short, approximately 20 years under normal working conditions. In wind farms, the turbine yield decreases due to the wind generated between the turbines, which hinders the movement of the turbines and thus reduces the amount of energy gained from the wind, which is a negative thing [13]. The energy produced by traditional turbines is less compared to WE, as the energy gained from the wind is related to the size of the turbine, and therefore the larger its size, the greater the energy gained, which is a negative matter that makes it difficult to complete these giant turbines and increases the costs [14]. Also, giant turbines require complex technologies and high-quality materials, which is difficult at present. To overcome these

disadvantages, the use of multi-rotor turbines has been proposed as an effective solution to increase the yield and overcome the wind generated between the turbines in wind farms [15]. Also, to meet the increasing energy demand and reduce the bill of production, transportation, and energy consumption. These turbines have been studied in several works [16], [17], [18], [19], and all of these works have shown their importance in increasing the energy gained from the wind. Also, these turbines withstand strong winds and are characterized by stability, which makes them the most suitable in the field of generating energy from wind. In addition to wind turbines, electrical machines called generators are used. Their role lies in converting the energy gained from the wind into current. Several types of generators can be used to convert this energy.

Currently, the doubly-fed induction generators (DFIGs)-based WEGs with the variable-speed are the most popular generators used in WEGs [20]. Their primary benefit is possessing static converters with 3-phases, which are proposed for a part of the nominal power of DFIG [21]. This makes DFIG cost-effective compared to recent existing conversion systems solutions (such as permanent magnet synchronous machines (PMSMs) and hybrid excitation synchronous generators). The synchronization speed of the DFIGs is within a $\pm 30\%$ range when operating, thus guaranteeing the reduction of the static converters dimensioning values, as they are linked between the winding of the DFIG rotors and grid [22]. Moreover, DFIG is considered to be highly durable, low maintenance, low cost, and easy to control compared to many generators, making it the most suitable in the field of wind energy [23]. In energy systems that rely on the use of DFIG, the network is connected directly to the fixed part of the DFIG, and its moving part is connected to the network using two inverters that are different in principle and operation. The grid side inverter is called a grid side converter (GSC), as its role is to convert alternating voltage into direct voltage. The inverter on the automatic side is called the rotor side converter (RSC), where the role is to convert the voltage generated by the GSC into an alternating voltage of a lower value than the grid voltage to feed the generator and control its speed and thus the resulting energy [24]. To control the DFIG, the RSC and GSC must be controlled, and therefore two controls are used, as these two controls can be of the same type or different. Mostly, GSC is used by an uncontrolled inverter to smooth systems and reduce costs, and only RSC is controlled [25]. Many control strategies have been adopted to control capacities, as these strategies differ in principle, simplicity, ease of completion, performance, durability, cost, and ease of completion. These strategies have been classified according to the work done in [26] into four families, where the first family represents linear controls and the second family represents non-linear control strategies that differ from the first family in terms of performance, principle, and robustness. The third family is the family of intelligent controls that rely on artificial intelligence, where neural networks, fuzzy logic (FL), and genetic algorithms (GAs) can be found. These strategies are relied upon to determine control gain values and therefore provide effective solutions, and simplicity and ease of use are among their most prominent features. The fourth family is the hybrid control family, where previous families are relied upon to create this family. Hybrid control strategies are a combination of various controls to obtain a new control characterized by high performance, great durability, and effectiveness in improving the characteristics of the systems.

Traditionally, the vector command (VC) strategy is considered one of the most prominent strategies previously used to control DFIG [27], as it relies on the use of a proportional-integral (PI) controller in order to control the characteristic quantities. In this control strategy, pulse width modulation (PWM) is used to generate operating pulses in the RSC of DFIG, where the voltage reference values generated by the PI controllers are converted into pulses. This strategy depends on knowledge of the mathematical model of DFIG, which makes it complex and is affected if the system parameters change [28]. This strategy is of two types: the direct VC (DVC) strategy [29] and the indirect VC (IVC) strategy [30], and the difference between them lies in the number of controllers used, performance, and durability. According to the work done in [31], the DVC strategy is considered easy to implement, inexpensive, and simple compared to the IVC strategy. However, the IVC strategy is characterized by high performance, great durability, and quick dynamic response compared to the direct strategy. Also, the IVC strategy underestimates the power ripple and total harmonic distortion (THD) compared to the direct strategy [32]. A researcher has used the DVC technique in [33], which uses fuzzy-space vector modulation (FSVM) to command and control the DFIG-based WE system. In this strategy, a two-level FSVM was used to generate the pulses needed to operate the RSC. The GSC was used with diodes to reduce the degree of complexity and demonstrate the effectiveness of the FSVM strategy in improving the quality of the current. The Matlab environment was used to implement the proposed strategy and study it with the traditional strategy. The simulated results showed that using the FSVM strategy has a positive effect on the quality of current and power. In [34], the IVC method is suggested to regulate and command the power of the DFIG integrated into the WEs. In this work, the author applied the IVC strategy only to the RSC, where he used the modified SVM strategy to generate the necessary operating pulses. This strategy was applied to a 1.5 MW DFIG using a variable wind speed in a MATLAB environment. The simulation results showed that this strategy has satisfactory performance but with ripples at the power and current levels, especially in the durability test, which is negative.

In the families of linear controls, direct torque command (DTC) is considered the most prominent and widespread family in the field of controlling electrical machines due to the ease and simplicity that distinguishes them from other controls [35]. In this strategy, hysteresis comparators (HCs)

are used to control both the torque and flux of the electrical machine and the outputs of these controllers are used as inputs to a conversion table through which the operating pulses of the inverter are generated. The researchers in [36], have designed a DTC technique to regulate and command the flux and torque of DFIG-WEG. In this work, the DTC strategy was applied as a suitable and effective solution to control the RSC, as this strategy needs to estimate both torque and flux in order to calculate the error in torque and flux, which makes the DTC strategy affected in the event of a malfunction in the machine, which is undesirable. In addition, this strategy has a fast dynamic response, as proven by the simulation results obtained using the Matlab environment. In the completed durability test, a noticeable increase in the value of THD of current and power ripples is observed, which is a negative indication of a decrease in the quality of current and power. In [37], the authors suggested the DTC strategy based on second-order continuous sliding mode controllers (SOCSMC) to control the RSC of a 1.5 MW DFIG-based wind turbine system. A SOCSMC control was used to control the characteristic amounts, and the outputs of these controls are reference voltage values. The latter were used as inputs to the SVM strategy in order to generate operating pulses for the RSC, where simplicity and ease of implementation are among the most prominent features of this control. Compared to the traditional DTC strategy of the DFIG, the nonlinear DTC technique is more reliable, where the flux and torque ripples are minimized, and the quality of energy is lessened. Despite the performance of SOCSMC, ripples remain present at the level of power, torque, and current, especially in the case of durability testing. An increase in the ripple values and the THD of current is observed. The backstepping command (BC) was suggested to command the flux and torque of the DFIGs rotor [38]. In this work, the BC strategy was used to convert the error in power to reference values in voltage, as this strategy is considered robust and has satisfactory performance. However, this strategy has drawbacks and problems. It is considered a complex strategy, expensive, difficult to implement, and contains a significant number of gains, which makes it difficult to control the dynamic response. Also, this strategy depends on the mathematical model of the machine, which makes it give unsatisfactory results in the event of a malfunction in the machine. Moreover, in this strategy, capacity estimation is used, which makes it affected, which is negative. This strategy was implemented in a MATLAB environment using variable wind speed to study the behavior and compare it with the traditional strategy, where the numerical simulation results show the characteristics of the suggested command to reduce and minimize the supplied active and reactive powers (Ps and Qs) ripples and ameliorates the currents/powers quality compared to the DVC technique. A direct power command (DPC) for DFIG has recently been suggested [39], where this strategy has the same structure, principle, and simplicity as the DTC strategy, with the only difference between them being the controlled amounts. In this strategy, a two-level HC is used to control the reactive power (Qs), and a three-level HC is used to control the active power (Ps), while using a state table to generate the necessary pulses necessary to operate the inverter.

Nevertheless, the DPC technique has several advantages: robustness against machine parameter mismatch, computational simplicity, and fast dynamic response [40]. However, the energy ripples and the high value of the THD of supplied DFIG currents are the main drawbacks of the DPC technique [41]. Also, the DPC strategy is affected by the change in machine parameters due to the presence of power estimation, which allows for higher ripple values and lower current quality, so several solutions have been proposed to overcome these problems and drawbacks. In [42] the authors suggested the DPC technique based on an estimated flux. This strategy differs from the traditional DPC strategy, as flux estimation was used as a suitable solution to increase performance and overcome problems. The MATLAB environment was used to implement the proposed strategy, comparing the behavior of the proposed strategy with that of the traditional strategy. The results showed that there was a noticeable improvement in the system's performance if the proposed strategy was used, and a noticeable decrease in the value of THD of current. However, the quality of power and current remains present, along with the problem of estimating flux, which is related to measuring voltage and current, which requires the use of high-precision measuring devices to reduce error. In [43], it was proposed to utilize a new DPC technique that is based on the flux-oriented control (FOC) with a fixed switching frequency. This FOC-based DPC strategy is complex, difficult to implement, expensive, and has a significant number of gains. Also, using the FOC strategy to improve the performance of the DPC strategy makes this strategy linked to the mathematical model of the system, which is a negative thing that contributes to increasing the ripples in the event of a malfunction. However, the simulation results showed that there is an improvement in the characteristics of the DPC strategy in the case of using the FOC strategy with the presence of ripples at the level of torque, power, and current, which is undesirable. In [44], the researchers propose a novel DPC technique based on the fuzzy technique to command the DFIG-WEGs. In this proposed solution, the FL technique was used to replace traditional controllers and state tables, as using this solution is not related to the mathematical model of the machine, which allows for better results. The use of the FL technique is based on experience and is characterized by high robustness against internal and external influences of the system. The negative of this proposed control is the lack of mathematical rules that allow defining the FL rules necessary to obtain good results and using them to estimate capacities, which allows for raising the ripple value and the THD value in the durability test. However, this proposed DPC-FL strategy gave many advantages such as reducing the torque ripple, reducing the overshoot value, and reducing the THD voltage.

In [45], the researcher suggests a new DPC strategy based on neural NSVM strategy to command the RSC of a DFIG-based wind turbine system. The DPC-NSVM strategy is different from the traditional strategy in terms of structure and principle and uses the same estimation equations. The DPC-NSVM strategy is characterized by high durability, easy implementation, fast dynamic response, and outstanding performance in reducing power and torque ripples. The MATLAB environment was used to implement this strategy on a variable-speed 1.5 MW DFIG. The graphical and numerical simulation results show the superiority of the DPC-NSVM strategy over the traditional strategy in improving the characteristics of the studied energy system. Recently, the twelve sectors of the DPC technique based on neural HCs were proposed [46]. In this work, the author used neural networks to replace traditional controllers and used a state table to generate operating pulses for an RSC of 1.5 MW DFIG, where the proposed control has the same structure as the traditional strategy. This proposed strategy was implemented in a Matlab environment using variable wind speed to study the proposed control behavior, where the results showed a noticeable improvement in the value of power and torque ripples compared to the traditional strategy. However, the quality of current and energy remains present in this strategy due to the presence of capacity estimation, as in the durability test, an increase in the values of ripples and THD of current is observed, which is negative. Moreover, the DPC strategy based on artificial neural networks (ANNs) is suggested to command the DFIG-WEGs by the integration of the neural PWM (NPWM) technique [47]. In this work, the author used an ANN to generate voltage reference values based on error powers, and an ANN-type control was used for this purpose. Also, the PWM strategy based on the ANN controller was used to generate the necessary operating pulses for the RSC of 1.5 MW DFIG. The proposed control is characterized by high durability, outstanding performance, simplicity, inexpensive, and easy to implement. This proposed solution is based on estimating capabilities and on experience in determining the number of neurons in each layer, as the MATLAB environment was used to implement it. The results obtained indicate that the quality of the current and power increased significantly compared to the traditional strategy in all tests performed. In [48], the researchers combined the DPC technique with the SVM strategy to command and control the supplied energy and torque of a permanent magnet synchronous generator. In addition to using the SVM strategy, a PI controller was used to control the capabilities, as the simplicity and ease of implementation enjoyed by the traditional strategy was maintained. This strategy was implemented in a MATLAB environment using variable wind speed, where the results showed that the quality of the current, the overshoot value, steady-state error (SSE), and response time are low in the case of the proposed strategy compared to the traditional strategy. However, in the durability test, it is noted that the ripples increased in value, which is negative. In [49], the sliding mode control (SMC) technique was suggested in order to ameliorate the performances of the DPC technique for DFIG-WEGs. Using the SMC strategy increases the durability and performance of the DPC strategy, which increases the quality of current and power. But using the SMC strategy increases complexity and makes the DPC strategy related to the mathematical model of the machine, which is a negative thing that increases the ripples and the value of the THD of current if the machine parameters change. The simulation results show the outstanding performance of the proposed control in all completed tests, noting that there is an impact if the machine parameters are changed as a result of using power estimation. The DPC technique and BC technique are combined to improve the current quality of the DFIG [50]. The BC technique was used to compensate for traditional controllers, as the outputs of this strategy are the reference voltage values. The latter are inputs to the PWM strategy, where these reference values are converted into pulses to operate the RSC of DFIG. Therefore, using the BC technique increases complexity and makes the DPC strategy difficult and expensive to implement. Also, using the BC technique increases the number of gains in the DPC strategy, which is a negative matter that makes it difficult to control the dynamic response to capabilities. Another negative of this proposed strategy lies in its use to estimate capabilities, as the same equations found in the traditional strategy are used. The results obtained using MATLAB showed that the proposed technique has effective performance and great effectiveness in improving the characteristics of the studied system compared to the traditional DPC strategy. In [51], the author proposed a new strategy for DPC of 1.5 MW DFIG based on the use of both the PWM and terminal synergetic controller (TSC) strategies, where simplicity, efficiency, simplicity, durability, distinguished performance, low cost, and ease of implementation are the most prominent features of this strategy. proposed. In this proposed strategy, a TSC control was used to control the power, where the outputs of these controls are the reference values of the voltage. The negative of this strategy lies in its use of estimating capabilities, which is a negative thing that helps reduce the quality of power and increase the value of THD of current. Using MATLAB, the proposed control was implemented and compared with the traditional strategy in terms of reference tracking, robustness, ripple reduction ratios, THD, overshoot, and SSE value. The numerical and graphical results demonstrate the superiority of the proposed strategy over the traditional strategy in improving system characteristics. Another nonlinear technique is suggested to ameliorate the characteristics of the DPC strategy in [52], where the third-order SMC strategy is used to replace traditional controllers. The third-order SMC strategy is a development of the traditional SMC strategy, as its use contributes to increasing the performance and durability of the DPC strategy. In the latter, a third-order SMC control was used to control the power, and the PWM strategy was used to convert the voltage reference values resulting

from the third-order SMC strategy to the operating pulses in the RSC. Using a third-order SMC strategy increases complexity and implementation costs compared to the traditional strategy, which is undesirable. Using the third-order SMC strategy increases the number of gains, which makes it difficult to determine the optimal values for these gains and to obtain good results. Simulation results show that the results were better when using the third-order SMC strategy compared to the traditional strategy. SC and SMC techniques are combined to regulate the *Ps* and *Qs* of the DFIG controlled by the DPC strategy [53]. This proposed strategy is different from the above works in terms of principle, structure, and performance. The DPC method based on SC-SMC controllers is more robust than the DPC technique. In this proposed control, a PWM strategy was used to convert the voltage reference values generated by the SC-SMC controller into operating pulses for the RSC of 1.5 MW DFIG. This proposed strategy is simple, inexpensive, easy to implement, and has high performance with great durability. This is demonstrated by the results obtained using the MATLAB environment. The use of a SC-SMC controller led to an increase in the quality of current and power while reducing the values of both response time, SSE, and overshoot compared to the traditional DPC technique. In the works [54], [55], a proposal for new linear controls relied upon using both a PI controller and a proportional-derivative (PD) controller to improve the characteristics of the DPC strategy of 1.5 MW DFIG-MRWT, where the PWM strategy was used to simplify the system and reduce the cost of implementation. In these works, controllers of the form PD(1+PI) and PI(1+PI) were used to control the power, as using these controllers increased the number of gains compared to using the PI controller. These proposed controls, were implemented in the MATLAB environment using different forms of WS, and the results obtained show the extent of the effectiveness of these strategies in improving the characteristics of the studied energy system compared to the traditional strategy. These strategies have the disadvantages of higher ripples, response time, THD of current, SSE, and overshoot in robustness testing as a result of using power estimation. Several scientific works were proposed in [56], [57], [58], [59], and [60] based on the use of new strategies, where genetic algorithms and the particle swarm optimization (PSO) technique were used to determine the values of gains in some of these controls to increase performance and durability. These proposed strategies are characterized by high durability and effective performance in improving current quality and reducing power ripples. The MATLAB environment was used to implement these strategies, and a 1.5 MW DFIG was used to accomplish these tasks. The results obtained show the high performance of these strategies compared to the traditional strategy. Experimental work on a new strategy was completed in [61], where a feedback PI controller was used to increase performance and improve the quality of the current. The proposed control is simple, effective, robust, has excellent performance, and few gains, easy to implement, and inexpensive. First, this proposed strategy was implemented in a MATLAB environment using a variable wind speed, and this strategy was applied to a 1.5 KW DFIG. Secondly, this proposed strategy was implemented experimentally using dSPACE 1104, where the experimental results confirm the obtained simulated results. Experimental results confirm that the use of a feedback PI controller contributes to increasing power quality and reducing the value of THD of current compared to a traditional controller. However, in the durability test, it is observed that the ripples rise and the quality of the current decreases, which is negative. In [62], the authors used a combination of both neural networks and fractional-order control to obtain an effective and robust controller to overcome the defects and problems of the DPC of 1.5 MW DFIG-MRWT strategy. The principle of this proposed strategy is almost the same as the principle used in the work [63] with a difference in the smart strategy used, as in this work a combination of FL technique and fractional-order control was used. These proposed controls are new effective solutions based on changing the structure of the traditional strategy while using the same estimation equations. In these controls, the PWM strategy was used to generate the control pulses necessary to operate the RSC of 1.5 MW DFIG-MRWT. These strategies were implemented in the Matlab environment under different working conditions, where the graphical and numerical results showed high performance and great robustness compared to the traditional strategy. In [64], the super-twisting sliding mode control (STSMC) and SC technique are combined to ease the DPC technique characteristics of the DFIG-WEG. In this work, an SC-type control was used to control the power and generate voltage reference values. In addition, the maximum power point tracking (MPPT) strategy was used to obtain the reference value for active power. This proposed strategy relies on estimating capabilities, which makes it slightly affected if the machine parameters change. This strategy was implemented in a MATLAB environment using different tests, and the results obtained show that the quality of current and power is better when using the proposed strategy compared to the traditional strategy. The STSMC strategy is considered one of the simplest and easiest to implement nonlinear strategies, as this strategy has effective performance and great durability. Using this strategy leads to significantly improving the characteristics of the systems. In [65], a GA strategy was used to calculate STSMC gains to control a photovoltaic system, where experimental results showed the distinctive performance of this strategy in reducing energy ripples, THD value of current, overshoot, and SSE. Another smart strategy, represented by PSO, was used in [66] to improve the characteristics of the STSMC strategy of DFIG. The proposed strategy is characterized by simplicity, outstanding performance, great durability, and ease of implementation. The results obtained from the MATLAB environment show that the power quality is high when using this strategy compared to the traditional control. In [67], fractional-order control was

used to improve the characteristics of the STSMC strategy of the DFIG, as the proposed strategy is characterized by simplicity, ease of implementation, and high robustness. The use of this proposed strategy led to improving the characteristics of the studied energy system, and this is confirmed by the simulation results obtained compared to the traditional strategy. In [68], PI, STSMC, and fractional-order control were combined to obtain a new controller characterized by strong and effective performance in order to increase the quality of power generated by DFIG. This proposed controller is characterized by high performance, as the MATLAB environment was used to implement it and compare it with the traditional controller. The numerical and graphical results showed that using this proposed controller has high performance and great durability compared to the traditional controller. Several new strategies for the STSMC technique have been proposed as suitable and effective solutions to increase the durability and performance of energy systems [69], [70], [71], [72], [73], [74], [75], [76], [77], [78], [79], [80], as these solutions differ in terms of durability, performance, simplicity, and ease of implementation. These proposed solutions were implemented in the Matlab environment with a study of the behavior compared to the behavior of traditional control based on traditional controllers. The results obtained show the satisfactory performance of these solutions in terms of increasing the durability and performance of the systems. All of the work mentioned above is work that was completed using simulation only, where the MATLAB environment was used to verify the validity of the proposed strategies. Power quality, THD value of current, overshoot, SSE, response time, durability, and performance are almost the most prominent negatives found in these proposed solutions. As is known, energy quality is one of the most prominent features that must be focused on and paid attention to. The quality of power and current is related to the type of proposed control strategy and the extent of its ability to improve the characteristics of the studied energy system. Therefore, it is necessary to choose a control strategy with high characteristics in order to obtain excellent results.

In this work, a new DPC strategy for DFIG-WEG is suggested. The developed command relies on the use of the combination between STSMC and neural networks to control the *Ps* and *Qs* of DFIG-WEG and to generate the necessary reference values to operate the RSC of DFIG. Neural STSMC (NSTSMC) is a controller characterized by effective performance in reducing ripples and increasing the quality of the current, as it is characterized by durability, simplicity, and ease of implementation. Besides using NSTSMC, the space vector pulse width modulation (SVPWM) strategy is used to convert reference values into operating pulses for the RSC of DFIG. The newly suggested DPC-NSTSMC-SVPWM technique ensures the advantages of the traditional DPC strategy such as simplicity, fewer parameters dependence, and fast response times by the control systems. The stability of the DPC-NSTSM-SVPWM technique is fully guaranteed using the Lyapunov stability strategy. So, the DPC-NSTSMC-SVPWM technique is one of the main contributions of this paper, as it is confirmed by simulation and experimental work. In this proposed strategy, GSC was used by an uncontrolled inverter to simplify the studied energy system and demonstrate the extent to which the proposed strategy is capable of improving the quality of current and power without resorting to using GSC control. First, this proposed strategy was verified using the Matlab environment and by comparing its behavior with the DPC-STSMC strategy under different working conditions. The numerical and graphical results showed the high performance and effectiveness of the proposed strategy in improving the characteristics of the energy system compared to the DPC-STSMC strategy. Secondly, the dSPACE 1104 card is used to immediately implement the proposed new strategy and verify its validity and its ability to improve the characteristics of the energy system in the case of variable wind speeds. The obtained experimental results are compared with the DPC-STSMC strategy. Accordingly, the experimental work of this proposed strategy is one of the most prominent main contributions of this paper. The objectives achieved from this completed paper can be summarized in the following basic points:

- Reducing power and current ripples compared to the DPC-STSMC strategy;
- Increasing the performance of the energy system based on wind speed compared to the DPC-STSMC strategy;
- Reducing the THD of current compared to the DPC-STSMC strategy;
- The proposed strategy is experimentally validated and confirms the simulation results significantly;
- Significantly overcome the drawbacks and problems of the traditional strategy (DPC technique);
- Improving and increasing the resiliency and durability of real wind power and energy generation systems.

The work was divided into 6 different sections, where the mathematical model of a system was given in the second section. In the third section, explain the proposed control by mentioning the pros and cons. Simulation results by MATLAB are presented in Section IV. The fifth section offers the experimental work done with the results. The conclusions of the work are explained in the last section.

II. WP SYSTEM

The energy system studied in this section has great importance in reducing production costs and electrical energy consumption compared to traditional systems. Also, it contributes greatly to protecting the environment and reducing temperature rise, as it is considered an environmentally friendly system. The studied energy system is characterized by simplicity, low cost, and ease of implementation. In Figure 1 a general model of WEGs based on DFIG is illustrated. To study and implement this system, it is necessary to know the main sections and mathematical modeling of this system, as this mathematical modeling is used for digital simulation [81].

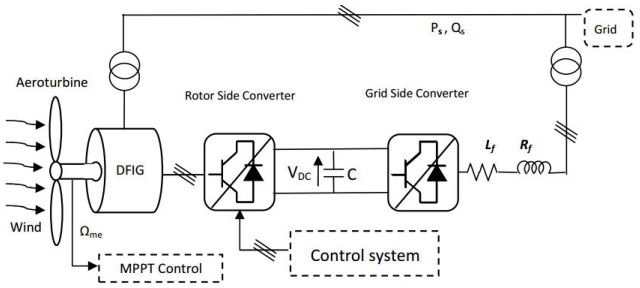

FIGURE 1. DFIG-WEG system.

The turbine, RSC, DFIG, and GSC are among the most prominent main sections of this studied energy system, as it is necessary to model both the turbine and the generator. As is known, the turbine is responsible for converting wind energy into mechanical energy, and the generator is responsible for producing energy. Therefore, the mathematical model for these two parts of the system must be known.

Equations of the mathematical turbine model are given and presented as follows [50]:

$$\begin{cases} P_{Rotor} = P_{wind}.C_p(\lambda, \beta) \\ P_{wind} = 0.5\rho A v^3 \\ T_{Rotor} = \dfrac{P_{Rotor}}{\Omega_t} \end{cases} \Rightarrow \begin{cases} P_{Rotor} = 0.5\rho A C_p.v^3 \\ T_{Rotor} = \dfrac{1}{2\Omega_t}\rho S.C_p v^3 \end{cases} \tag{1}$$

With:

$$\begin{cases} C_p(\lambda, \beta) = k_1(\dfrac{k_2}{A} - k_3\beta - k_4)e^{(\frac{-k_5}{A})} + k_6\lambda \\ k_1 = 0.5872, \mathrm{k}_2 = 116, \mathrm{k}_3 = 0.4, \mathrm{k}_4 = 5, \mathrm{k}_5 = 21 \\ and\ \mathrm{k}_6 = 0.0085 \end{cases}$$

The energy produced by turbines is related to the change in wind speed, as the higher the wind speed, the greater the energy gained, and vice versa. Also, the dimensions of the turbine have an impact on the amount of energy gained from the wind, as the larger the dimensions of the turbine, the greater the energy gained, and the smaller these dimensions are, the less energy gained.

Equation (2) expresses the mechanical part of the machine [82].

$$\begin{cases} T_{mec} = J\dfrac{d\Omega_{mec}}{dt} \\ T_{mec} = T_g - (T_{em} + f\Omega_{mec}) \end{cases} \Rightarrow J\frac{d\Omega_{mec}}{dt} = T_g - (T_{em} + f\Omega_{mec}) \tag{2}$$

Equation (3) represents the gearbox.

$$\begin{cases} \Omega_g = G.\Omega_t \\ T_{Rotor} = G.T_g \end{cases} \tag{3}$$

DFIG is considered one of the induction machines that is characterized by high performance and great durability, as it is low in maintenance and low in cost, making it the most suitable in the field of generating electrical energy from wind.

Also, the rotation speed and the resulting power can be controlled by controlling the feeding of the moving part, which gives an advantage not found in other machines. Moreover, this generator is easy to control and any control can be applied easily. The focus was on this generator in this work to generate electrical energy, and therefore it is necessary to know the mathematical model of this machine, as mathematical equations are given for the electrical and mechanical parts of this machine. To give the model of DFIG the Park transform is used, in which the corresponding electrical and mechanical equations are given [83].

Equations (4) and (5) express the electrical part of the machine.

$$\begin{cases} V_{sd} = R_s.\mathrm{I}_{sd} + \dfrac{d\varphi_{sd}}{dt} - \omega_s.\varphi_{sq} \\ V_{sq} = R_s.\mathrm{I}_{sq} + \dfrac{d\varphi_{sq}}{dt} - \omega_s.\varphi_{sd} \\ I_{sd} = \dfrac{1}{\sigma.L_s}.\varphi_{sd} - \dfrac{M_{sr}}{\sigma.L_r}.\varphi_{rd} \\ I_{sd} = \dfrac{1}{\sigma.L_s}.\varphi_{sd} - \dfrac{M_{sr}}{\sigma.L_s.L_r}.\varphi_{rd} \end{cases} \tag{4}$$

$$\begin{cases} V_{rd} = R_r.\mathrm{I}_{rd} + \dfrac{d\varphi_{rd}}{dt} - \omega_r.\varphi_{rq} \\ V_{rq} = R_r.\mathrm{I}_{rq} + \dfrac{d\varphi_{rq}}{dt} - \omega_r.\varphi_{rd} \\ I_{rd} = \dfrac{1}{\sigma.L_r}.\varphi_{rd} - \dfrac{M_{sr}}{\sigma.L_r.L_s}.\varphi_{sd} \\ I_{rq} = \dfrac{1}{\sigma.L_r}.\varphi_{rq} - \dfrac{M_{sr}}{\sigma.L_r.L_s}.\varphi_{sq} \end{cases} \tag{5}$$

Equation (6) represents the torque.

$$T_{em} = (\varphi_{rd}.\varphi_{sq} - \varphi_{rq}.\varphi_{sd})p \tag{6}$$

With:

$$\begin{cases} \varphi_{rd} = L_r.I_{rd} + I_{sd}M_{sr} \\ \varphi_{rq} = L_r.I_{rq} + M_{sr}.I_{sq} \\ \varphi_{sd} = L_s.I_{sd} + I_{rd}.M_{sr} \\ \varphi_{sq} = L_s.I_{sq} + M_{sr}.I_{rq} \end{cases}$$

Equation (7) represent the power of the DFIG.

$$\begin{cases} P_s = V_{sd}I_{sd} + V_{sq}I_{sq} \\ Q_s = V_{sq}I_{sd} - V_{sd}I_{sq} \end{cases} \tag{7}$$

A. PROPOSED DPC TECHNIQUE

The DPC technique is a linear command characterized by simplicity and ease of implementation. Also, it has a fast dynamic response and does not require knowledge of the mathematical model of the machine, which makes it give better results than several controls such as radial control [84]. This strategy relies on using the state table to generate trigger pulses in the RSC of DFIG, and therefore there are no internal loops in this strategy. In this command, two HCs are used to control and regulate the *Ps* and *Qs* of the DFIG [85]. The negative of this strategy lies in its use to estimate capabilities, which makes it linked to the parameters of the machine, especially the resistance Rs, as with the continuous operation

of the machine, this resistance changes, and thus there is an impact on the results and performance of the DPC strategy, which is negative. The DPC technique gives minimum energy ripples compared to the FOC, IVC, and DVC techniques [86].

Compared to predictive and BC techniques, the DPC technique gives more *Ps* and *Qs* ripples, and the THD value of the currents.

Several strategies were used to overcome the drawbacks of the traditional DPC strategy, as smart, nonlinear, and hybrid strategies were used as mentioned in the introduction. All of these solutions presented gave positive and negative results, which makes it necessary to always search for the best solution that can be applied in order to obtain good results. In this section, hybrid strategies are used as a suitable solution to surmount the drawbacks of DPC strategy and reduce supplied energy and current ripples. Also, the robustness of the system is greatly increased. To increase and strengthen the robustness of the system, the STSMC technique and ANN are combined in this work as an appropriate solution due to the characteristics of the two strategies, such as simplicity, where the resulting strategy is not related to the system parameters, and this is a good thing that gives satisfactory results. These two strategies were relied upon due to their advantages compared to other controls. As is known, neural networks are smart strategies that rely on experience and do not require knowledge of the mathematical model of the machine or system under study, as only the number of inputs and outputs is known. Also, neural networks are characterized by high performance and great durability against internal and external factors of the system, which makes them the most suitable in this work to reduce energy ripples and increase the quality of the current. Accuracy is also considered one of the biggest advantages of neural networks, which allows the characteristics of the systems to be greatly improved upon use.

The famous ANN technique is a mathematical model that was created using the concepts that exist in biological nerve systems as inspiration. Its goal is to simulate human mental capacities throughout the system, both in terms of machine and control behavior. Numerous nonlinear processing units, or neurons, are linked to one another in a neural network by synapses made of numerical values known as weights. These parts work together to efficiently get over the drawbacks of earlier technologies. They are organized into three layers: input, concealed, and output. The adaptability of this model to internal and external information passing via the network is one of its defining features. The following equation can be used to conceptually model the fundamental structure of a neuron:

$$y_i^{ANN} = f\left(\sum_i^n w_i x_i + b)\right) \tag{8}$$

The number of neural network inputs, the network outputs vector, the activation function, the neural network input vector, the weight matrix, and the bias are all indicated by the variables n, y_i^{ANN}, f, $x\{x_i, i = 1, 2, \ldots, n\}$, w_i and b respectively. Usually, the backpropagation approach is used

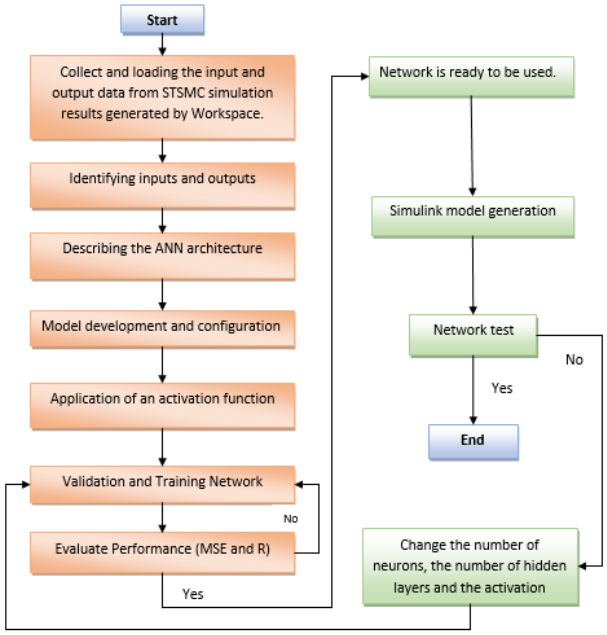

FIGURE 2. Diagram of the ANN controller training steps.

to update the weight matrix, and the bias input (the neuron's threshold or intercept) is either +1 or −1. The flowchart in Figure 2 provides a summary of the stages involved in creating an ANN technique.

The first step in creating the ANN technique is gathering and importing the datasets, as shown in Figure 2. The dataset used in this new proper work was imported from the STSMC method's simulation results generated by the workspace of MATLAB (R2021a).

As is known, neural networks are numerous and numerous, and several types can be used for this purpose. In addition, the use of neural networks is linked to learning algorithms, as several algorithms can be adopted to implement the neural controller.

The strategy proposed in this section differs from the controls mentioned above, as it is proposed to use a new NSTSMC method to control DFIG powers, as this strategy differs from the traditional DPC strategy. The NSTSMC strategy is used to generate reference voltage values from the power error, as there is one input and one output to the NSTSMC. On the other hand, the SVPWM strategy is used to generate the necessary pulses to operate the RSC of DFIG. The use of this DPC-NSTSMC-SVPWM strategy aims to improve the characteristics of the traditional strategy and increase the durability of the energy system. Also, improving the quality of the current if the machine parameters change. The new DPC-NSTSMC-SVPWM strategy is shown in Figure 3, where the robustness is a big one of the other advantages of this technique.

Compared to the IVC technique, the proposed strategy has outstanding performance, and great robustness, is easy to perform, has no internal loops, and is inexpensive.

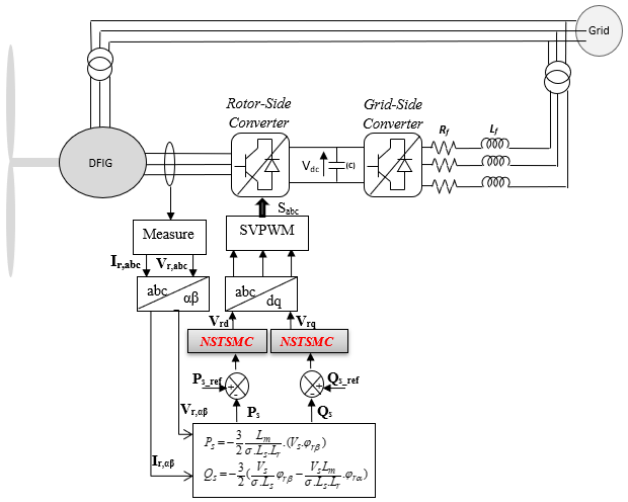

FIGURE 3. The DPC-NSTSMC strategy structure of DFIG.

The suggested DPC-NSTSMC-SVPWM strategy depends on capacity estimation to calculate the error, where the energy error is used as input to NSTSMC techniques. The estimation equations are the same equations used in the traditional DPC strategy and shown in the works [62], [63], where Equation (9) represents the estimation of capacities used in this work.

$$\begin{cases} Q_s = -\dfrac{3}{2}\left(\dfrac{Vs}{\sigma.Ls}\cdot\Psi_{r\beta} - \dfrac{Vs.Lm}{\sigma.Ls.Lr}\cdot\Psi_{r\alpha}\right) \\ P_s = -\dfrac{3}{2}\dfrac{Lm}{\sigma.Ls.Lr}\cdot(Vs.\Psi_{r\beta}) \end{cases} \tag{9}$$

STSMC strategy of the *Ps* and *Qs* is conceived to respectively change the q and d-axis voltages as shown in the Equations (10) [65], [66]:

$$\begin{cases} V_{dr} = K_1 \left|S_{Q_s}\right|^r \mathrm{sgn}(S_{Q_s}) + \overset{*}{V}_{dr1} \\ \overset{*}{V}_{dr1} = K_2 \mathrm{sgn}(S_{Q_s}) \\ V_{qr} = K_1 \left|S_{P_s}\right|^r \mathrm{sgn}(S_{P_s}) + \overset{*}{V}_{qr1} \\ \overset{*}{V}_{dr1} = K_2 \mathrm{sgn}(S_{P_s}) \end{cases} \tag{10}$$

where, $S_{Qs} = Q_{sref} - Q$ is the reactive power error,

S_{Ps}=$P_{sref} - P$ is the active power error.

In this proposed strategy, the reference value of active power is calculated using the MPPT strategy, and thus the value of active power becomes related to the shape of the wind speed change. The two constant gains k_1 and k_2 should prove the condition system stability. The Figure 4 show the structure STSMC- *Ps* and *Qs* command.

The following equations present a dynamic studied system withthe input u, the output y and the state x [65], [66], [67], [68]:

$$\begin{cases} \dfrac{dx}{dt} = a(x,t) + b(x,t)u \\ y = c(x,t) \end{cases} \tag{11}$$

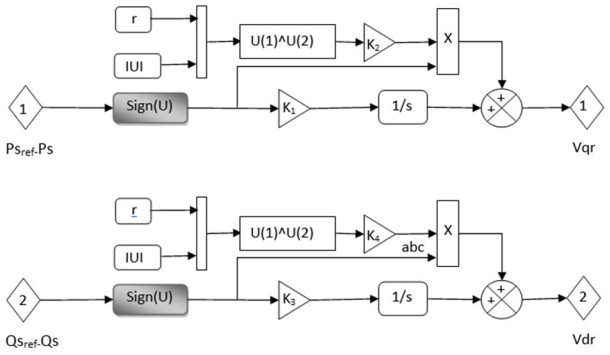

FIGURE 4. The STSMC- Ps and Qs techniques.

This command's difficulty is finding the input function u = f (y, $\dot{y}$) that can lead the system trajectories to the departure point y = $\dot{y}$ = 0 of phase planes, if possible in restricted times. The input "u" is specified as a new state variable, wherein the commutation command is carried out on its time derivative $\dot{u}_1$ [34].

The output of STSMC technique is related to the error (S), where S = y^* − y.

Equations (12) and (13) express the mathematical model and how to calculate the parameters, respectively [67], [68].

$$\begin{cases} u = |S|^r K_1 \mathrm{sgn}(S) + u_1 \\ \overset{*}{u} = K_2 \mathrm{sgn}(S) \end{cases} \tag{12}$$

$$\begin{cases} K_1 > \dfrac{A_M}{B_m} \\ K_2 \geq \dfrac{4A_M}{B_m^2}\cdot\dfrac{B_M(K_1 + A_M)}{B_m(K_1 - A_M)} \end{cases} \tag{13}$$

where, the upper and lower bounds of B and A in the 2nd derivative are represented by BM≥ B ≥ Bm and AM≥ |A|, [65], [68].

$$\frac{d^2y}{dt^2} = A(x,t) + B(x,)\frac{du}{dt} \tag{14}$$

ANN technique replaces the sign(u) to obtain NSTSMC technique. The suggested NSTSMC technique is robust, simple, and easy, in embedded system, to be implemented. The suggested NSTSMC technique minimizes the THD of supplied currents compared to the STSMC technique. Also, reduces the *Ps* and *Qs* ripples compared to the STSMC technique [39]. Figure 5 shows the NSTSMC technique of the *Qs* and *Ps* of the DFIG-based wind turbine.

The ANN technique is a type of smart command characterized by robustness and simplicity [62]. In the NSTSMC technique, 8 neurons in the hidden layer are employed. A single neuron is also used in the entry and exit layers. Figure 6 gives the ANN technique used to ameliorate and improve the performance of the STSMC *Qs* and *Ps* of the DFIG.

The Figure 7 shows the structure of the hidden layer of the ANN method.

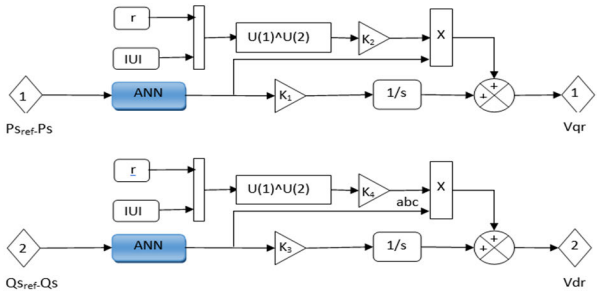

FIGURE 5. The NSTSMC command.

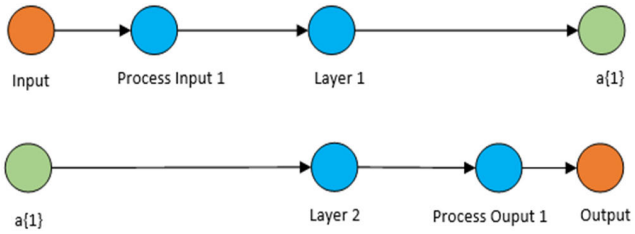

FIGURE 6. The ANN strategies.

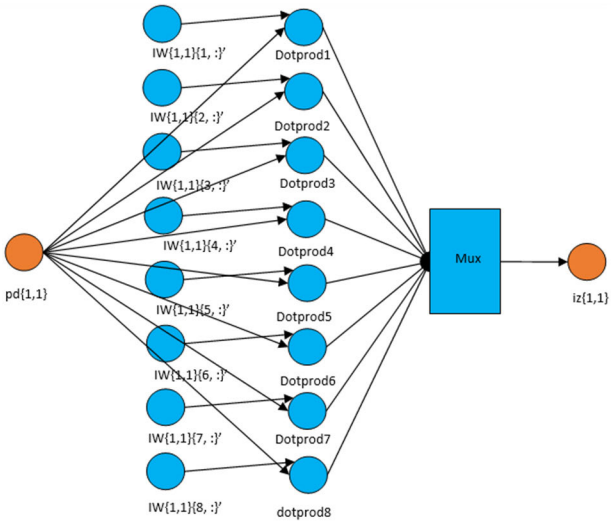

FIGURE 7. Hidden layer.

Accordingly, the properties of the neural network used to implement the two controllers corresponding to Ps and Qs control are represented in Table 1.

III. NUMERICAL RESULTS

A. SIMULATION TEST UNDER REAL WIND PROFILE

The simulation test of the DPC-NSTSMC strategy of the machine 1.5 KW DFIG-WEGs is compared with the DPC technique based on the classical STSMC controllers. Both control schemes were tested using the tracking reference test.

The used generator for simulations test has the following specific real parameters: $Pn = 1.5$ kW, $Vn = 398$ V,

TABLE 1. Characteristics of the neural algorithms.

Parameters	Value
Training	Levenberg-Marquardt algorithm
Coeff of acceleration of convergence(mc)	0.9
net.trainParam.goal	0
Number of neurons in hidden layer 1	8
Performances	Mean Squard Error (mse)
TrainParam.Lr	0.005
TrainParam.mu	0.9
Number of neurons in layer 1	1
TrainParam.goal	0
TrainParam.show	50
TrainParam.eposh	300
Number of neurons in layer 2	1

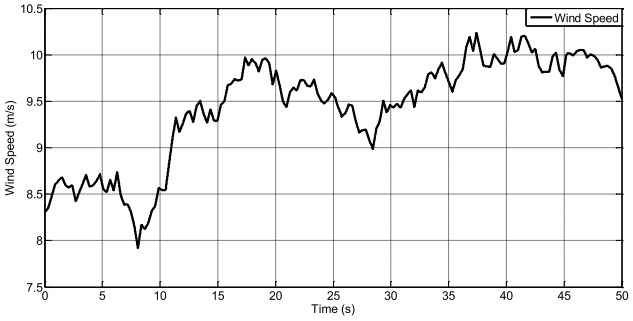

FIGURE 8. Wind speed profile.

$Rs = 1.18\ \Omega$, $f = 50$ Hz, Ls=0.20 H, $M = 0.17$ H, $Rr = 1.66\ \Omega$, $J = 0.04$ Kg.m2, $Lr = 0.18$ H, $fr = 0.0024$ Nm/s.

The obtained results are shown in Figures 8 to 21. Figure 8 represents the WS used to test the behavior of the DPC-NSTSMC-SVPWM technique, as the WS has a random shape. The effective power gained from the real wind is represented in Figure 9. This energy takes the form of changing the WS, as the value of the gained energy increases with increasing in the value of the WS. Also, the speed of the rotating part of the machine takes the forms of a significant change in the WS, as it is noted that the speed of the rotating part is related to the WS and its changes (Figure 10). Figure 11 is the tip speed ratio (TSR) of the turbine. It is noted that the TSR takes almost a constant value around 7.5 with presence of fluctuations and ripples, as these fluctuations are related to the strategy used to control the turbine (MPPT-PI technique). These ripples can be overcome by using smart or nonlinear strategies.

Figure 12 represents the Cp of the turbine, where the value of the Cp is not related to WS, but remains almost constant and takes a value of 0.49 with the presence of ripples. The *Ps* is represented in Figure 13. This *Ps* has a random shape for the two controls used in this work. Also, the change in the *Ps* takes the form of a change in the WS, as the value

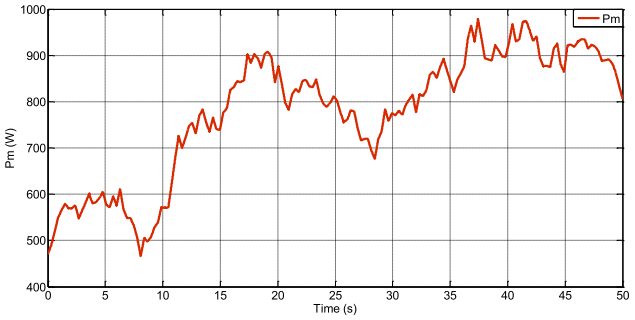

FIGURE 9. Mechanical power.

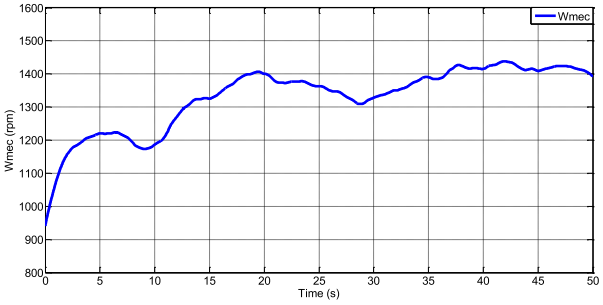

FIGURE 10. Mechanical angular speed.

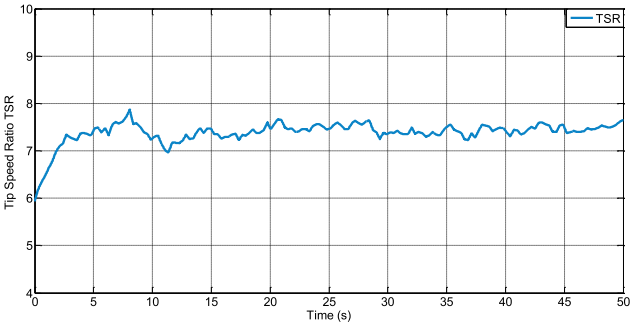

FIGURE 11. Tip speed ratio TSR.

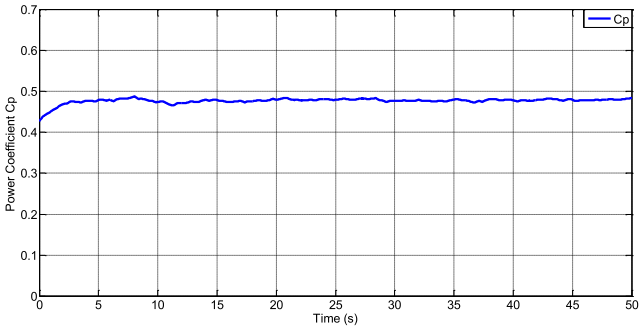

FIGURE 12. Power coefficient Cp.

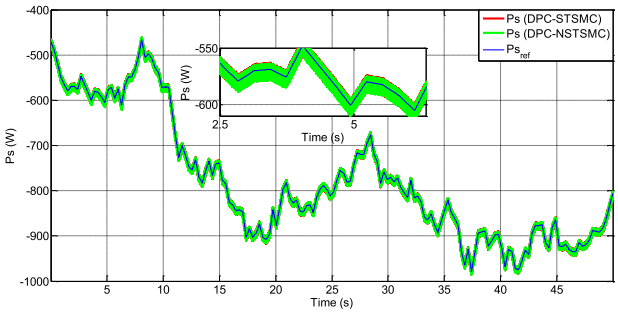

FIGURE 13. Active power Ps.

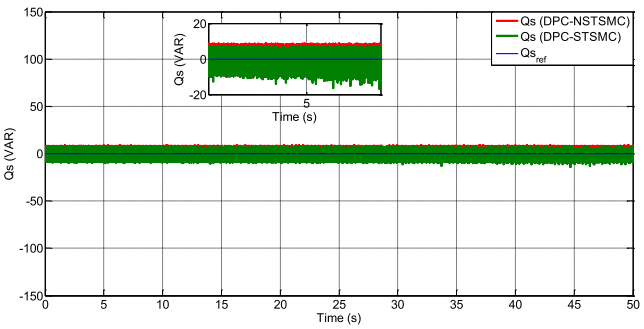

FIGURE 14. Reactive power Qs.

of the *Ps* increases with the value of the WS and vice versa. Also, it is noted that there are ripples and fluctuations at the level of *Ps*, and these fluctuations are larger in the case of the DPC-STSMC technique compared to DPC-NSTSMC-SVPWM technique. *Qs* are represented in Figure 14. This power is unaffected by the change in WS and remains equal to 0 VAR with ripples. The latter is greater in the event of DPC-STSMC technique in comparison to DPC-NSTSMC-SVPWM strategy.

Figure 15 represents a machine's power factor, where this parameter's value is 1 for the DPC-NSTSMC-SVPWM technique compared to the DPC-STSMC strategy. This last one, and at the moment 13 seconds, the parameter becomes not equal to 1, which is not desirable. However, the proposed control maintains the coefficient value equal to 1 throughout the simulation period. The torque is represented in Figure 16. The latter proves that the torque change is significantly associated with the WS change with the presence of fluctuations and ripples, where these ripples are less in the case of the DPC-NSTSMC-SVPWM technique compared to the DPC-STSMC technique. Figure 17 and Figure 18 represent the direct rotor currents and the quadrature rotor currents and of DFIG. It is noted from the two figures that the quadrature current changes according to a change in the *Ps* and the WS. The direct current is not affected by the change in WS and remains constant with the presence of ripples and fluctuations. The latter is greater in the case of the DPC-STSMC technique in comparison to the DPC-NSTSM technique.

Figures 19 and 20 represent the machine's rotor and stator currents. These currents are sinusoidal with ripples. However, in the case of the DPC-NSTSMC-SVPWM technique, the currents' shape is much better than the DPC-STSMC technique. Moreover, the change of stator currents and rotor

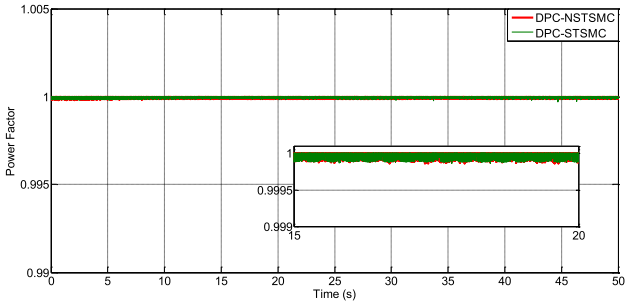

FIGURE 15. Power factor PF.

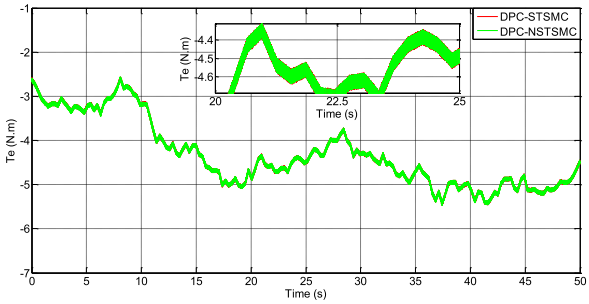

FIGURE 16. Electromagnetic torque Te.

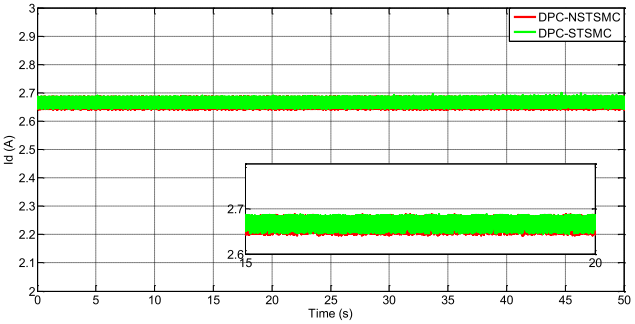

FIGURE 17. Direct rotor current Idr.

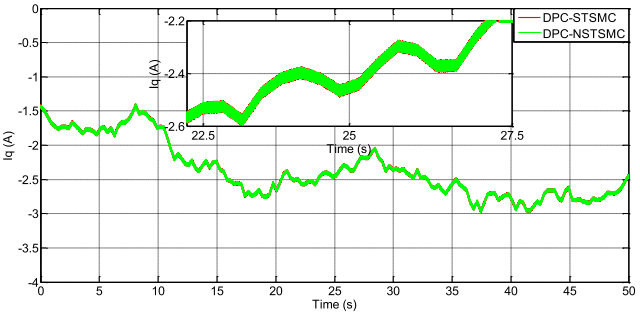

FIGURE 18. Quadrature rotor current Iqr.

currents takes the form of WS change for the two commands, and the ripples are less in the case of the DPC-NSTSMC-SVPWM technique than in the DPC-STSMC technique command. Figure 21 represents the THD of the currents (*Isa*) value for each of the two commands suggested in this recent research work. It is noted from the two figures that the DPC-STSMC technique gave a higher value than the DPC-NSTSMC-SVPWM technique, where the THD value was 1.07% and 0.83% for the DPC-STSMC technique and DPC-NSTSMC-SVPWM technique, respectively (see Figure 21). Accordingly, the DPC-NSTSMC-SVPWM technique reduced the value of the THD by an estimated rate of 22.42%. On the other hand, it is noted that the two controls have the same amplitude value of the signal (50 Hz) of current, which is positive for the proposed strategy. The numerical values for this test are represented in Table 2, where the values and percentages of reduction are given for response time, ripple, overshoot, and SSE of DFIG power. Through this table, the values of ripples, SSE, and overshoot of active power were reduced by percentages estimated at 10%, 50%, and 32.20%, respectively, compared to the DPC-STSMC strategy.

TABLE 2. Value and ratios of energy ripples, overshoot, SSE, and response time of both techniques for the first test wind real wind profile.

		Ps (W)	*Qs* (VAR)
DPC-STSMC	Ripples	15	18.3
	Overshoot	4.13	2.02
	SSE	8	10.10
	Response time	0.0054 ms	0.658 ms
DPC-NSTSMC-SVPWM	Ripples	13.5	16.10
	Overshoot	2.80	1.13
	SSE	4	6.23
	Response time	0.011 ms	0.89 ms
Improvement Ratios	Ripples	10 %	12.02 %
	Overshoot	32.20 %	44.06 %
	SSE	50 %	38.32 %
	Response time	-50.90 %	-26.06 %

For reactive power, the ripple, SSE, and overshoot values were reduced by 12.02 %, 44.06 %, and 38.32 %, respectively compared to the DPC-STSMC strategy. The proposed strategy provided an unsatisfactory turnaround time compared to the DPC-STSMC strategy. The latter reduced response time by rates estimated at 50.90 % and 26.06 % for both active and reactive power, respectively, compared to the proposed strategy.

B. ROBUSTNESS TEST UNDER REAL WIND PROFILE

In this test, the behavior of the proposed strategy is studied in terms of changing machine parameters compared to the DPC-STSMC strategy, where the same wind speed profile used in the first test is used. In this test, the values of the resistors and coils are changed, where the values of the resistors are multiplied by 2 and the values of the coils are divided by 2. The graphical results are represented in Figures 22 to 36. In Table 3 the numerical results obtained from this test are represented. Figure 22 represents the mechanical power resulting from the wind. It is noted that this power changes according to the change in the WS despite the change in the machine parameters. This is the same for the angular speed represented in Figure 23. In Figure 24 the tip speed ratios of the turbine are

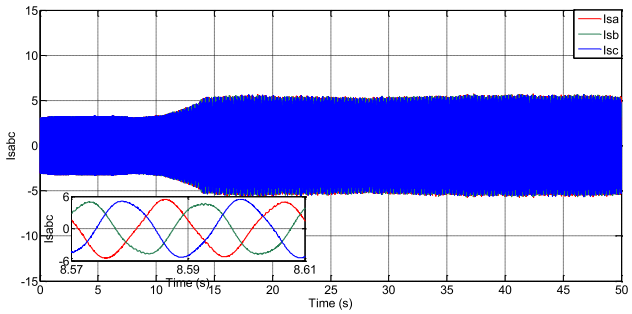

a) DPC-STSMC

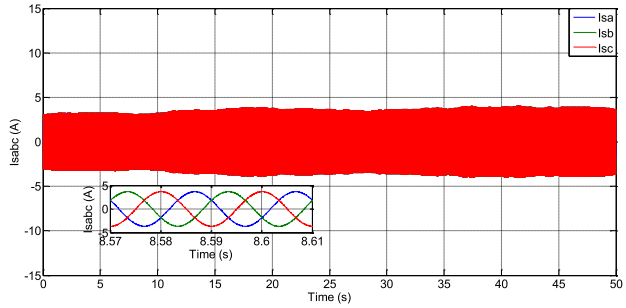

b) DPC-NSTSMC

FIGURE 19. Stator currents (Is_{abc}).

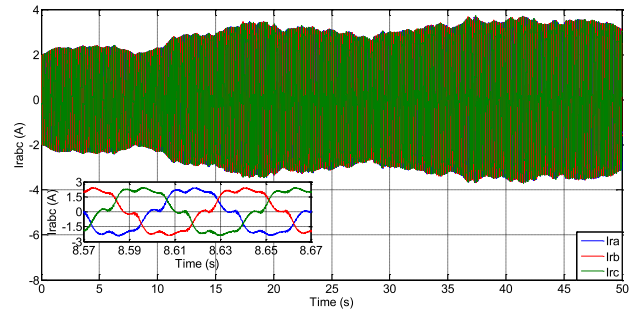

a) DPC-STSMC

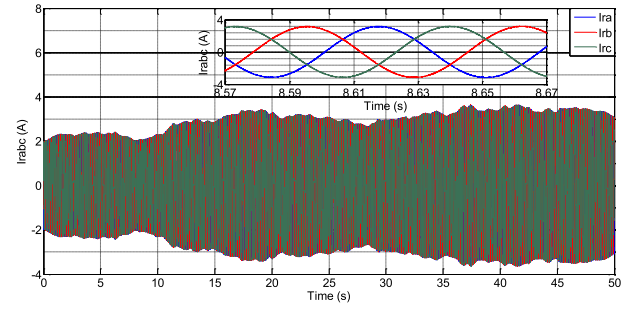

b) DPC-NSTSMC

FIGURE 20. Rotor currents (Ir_{abc}).

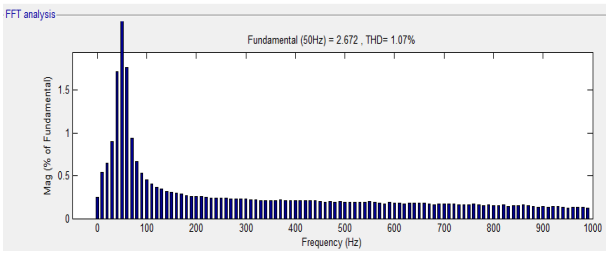

a) DPC-STSMC

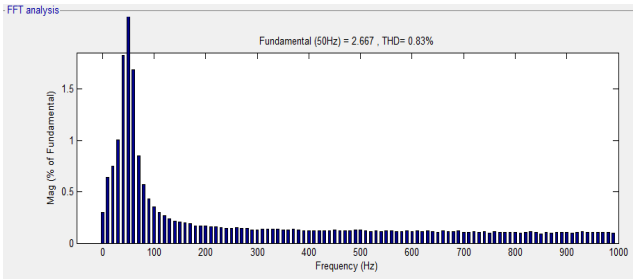

b) DPC-NSTSMC

FIGURE 21. THD of Isa.

TABLE 3. Value/ratios of energy ripples, SSE, overshoot, and response time of both techniques for the robustness test under real wind profile.

		Ps (W)	*Qs* (VAR)
DPC-STSMC	Ripples	17	19
	Overshoot	4.77	2.24
	SSE	10	12.6
	Response time	0.0064 ms	0.858 ms
DPC-NSTSMC	Ripples	16	17
	Overshoot	3.22	1.73
	SSE	6	7.3
	Response time	0.016 ms	1.2 ms
Improvement Ratios	Ripples	5.88 %	10.53 %
	Overshoot	32.49 %	22.77 %
	SSE	40 %	39.68 %
	Response time	-60 %	-28.50 %

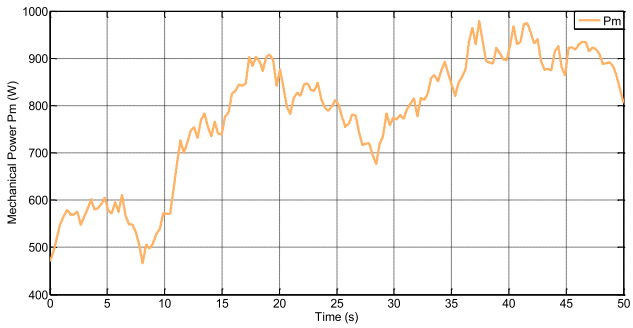

FIGURE 22. Mechanical power Pm.

shown, as its value is affected by the change in WS. These are the same results shown in the first test. In Figure 25, the power coefficient is given, where its value is close to 0.48 with ripples. These ripples are the result of using the traditional MPPT strategy.

In this test, the powers follow the references well, with ripples present (see Figures 26 and 27). The power remains constant and its value does not change according to the change in the shape of the WS, as it is noted that the undulations are larger in the case of using the DPC-STSMC strategy compared to the DPC-NSTSMC-SVPWM technique. However, the active power keeps changing according to the change in WS, and this is despite the change in the DFIG parameters. In Figure 28, the power factor is represented, where

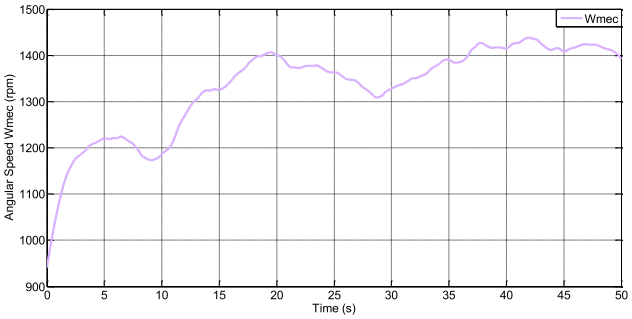

FIGURE 23. Angular speed.

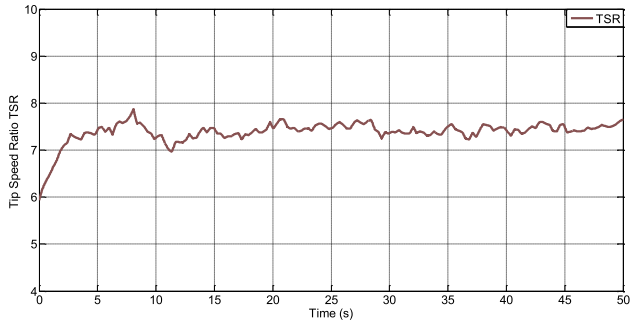

FIGURE 24. Tip speed ratio TSR.

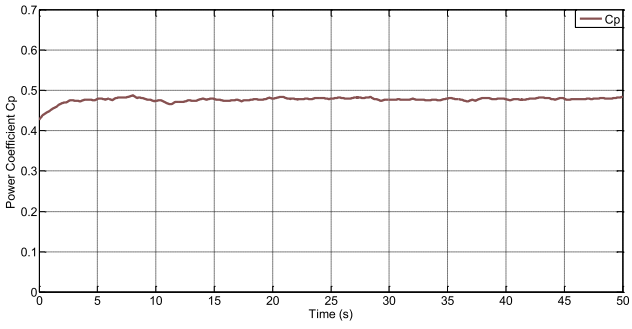

FIGURE 25. Power coefficient Cp.

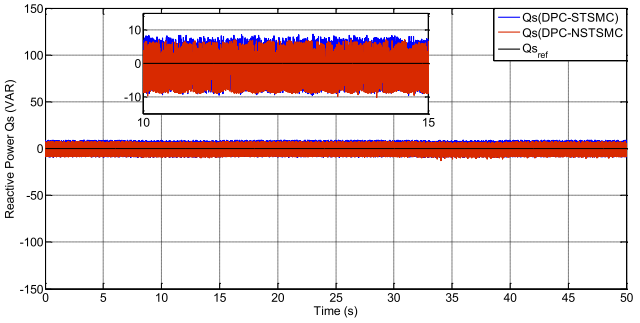

FIGURE 26. Reactive power.

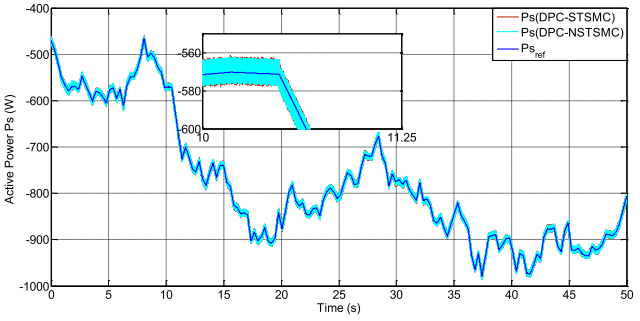

FIGURE 27. Active power Ps.

this factor takes a fixed value equal to 1 in the presence of ripples. These ripples are less in the proposed strategy, which is a positive thing despite the change in the machine parameters. The torque represented in Figure 29 takes the form of a change in WS and active power, where ripples are observed. The latter is less in the proposed strategy. In Figure 30 the shape of the current Id is represented, where its value remains constant with the presence of ripples. These ripples are less in the proposed strategy, with the shape of the change in this current being the same as the shape of the change in the reactive power. The shape of the change in the current Iq is represented in Figure 31. This current changes according to the change in WS, with large undulations in the case of the DPC-STSMC strategy compared to the proposed strategy. The stator and rotor currents are represented in Figures 32 to 35, where it is noted that these two currents have the same shape as the WS change. This current takes a sinusoidal shape with better quality if the proposed strategy is used compared to the DPC-STSMC strategy. The value of THD of current is represented in Figure 26, where its value was 1.30 % and 0.99 % for DPC-STSMC and DPC-NSTSMC-SVPWM, respectively. Through these values, the DPC-NSTSMC strategy gave a lower value compared to the DPC-STSMC strategy, as the value was reduced by an estimated percentage of 23.84 % compared to the DPC-STSM strategy. In addition, the two controls provide the same amplitude as the fundamental signal (50 Hz) of the current, and therefore the proposed strategy has satisfactory results that make it one of the strategies that can be relied upon in the future. The values and percentages of reduction of response time, ripple, overshoot, and SSE of DFIG power for the controls are represented in Table 2. The latter shows that the proposed DPC-NSTSMC-SVPWM strategy gave lower values for both ripples, overshoot, and SSE compared to the DPC-STSMC strategy and this is shown by the calculated reduction ratios. However, this proposed DPC-NSTSMC-SVPWM strategy provided unsatisfactory results compared to the DPC-STSMC strategy. The latter reduced the response time by an estimated percentage of 60 % and 28.50 % for both active and reactive power, respectively, compared to the proposed DPC-NSTSMC-SVPWM strategy.

In Table 4 the change in the THD value of current in the tests is shown. From this table, it is noted that the THD value increased in the second test compared to the first test for the two controls. This increase was estimated at +0.23 % and +0.16 % for both the traditional and proposed strategies,

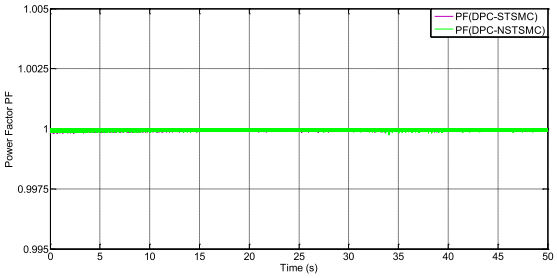

FIGURE 28. Power factor PF.

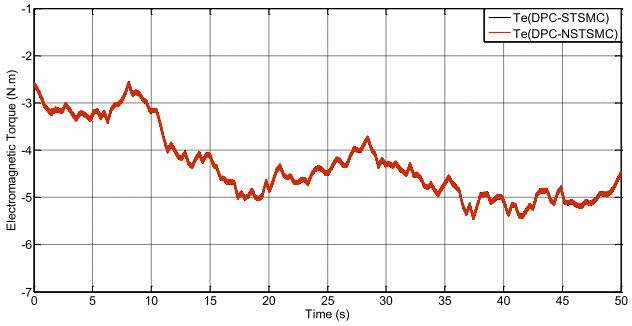

FIGURE 29. Electromagnetic torque.

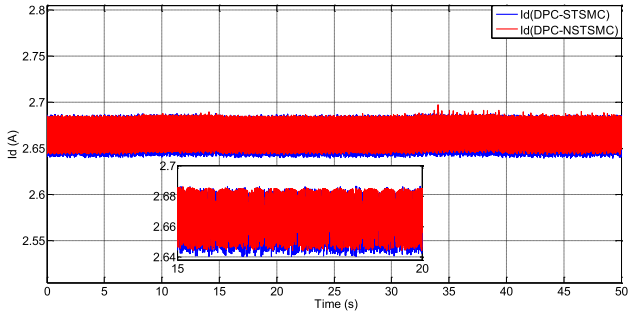

FIGURE 30. Direct rotor current I_d.

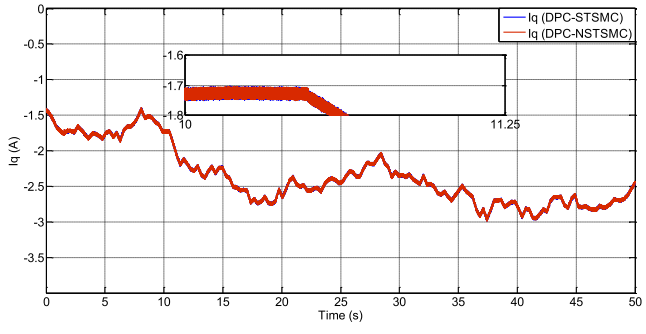

FIGURE 31. Quadrature rotor current I_q.

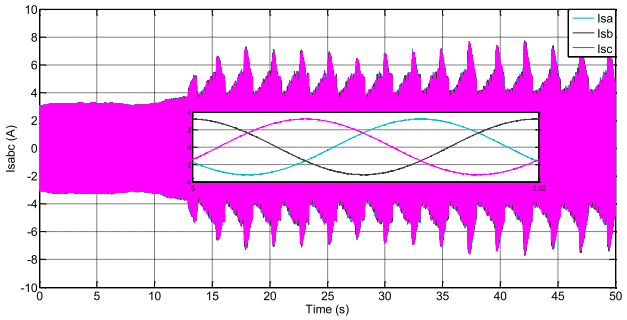

FIGURE 32. Stator currents Is_{abc} of DPC-STSMC.

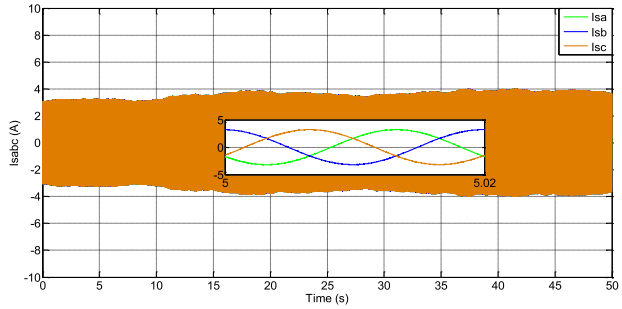

FIGURE 33. Stator Currents Is_{abc} of DPC-NSTSMC.

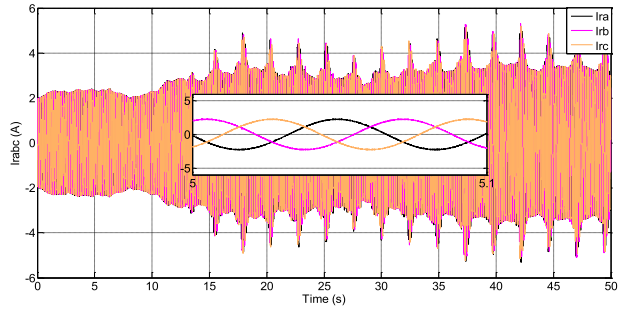

FIGURE 34. Rotor Currents Ir_{abc} of DPC-STSMC.

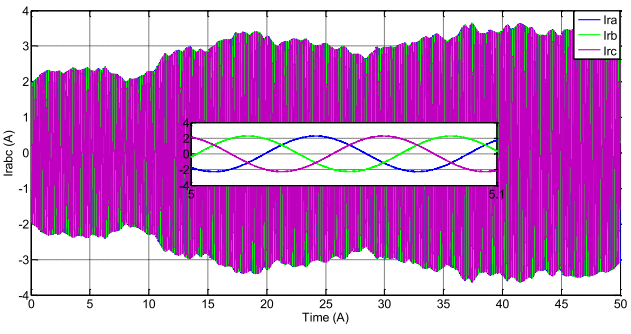

FIGURE 35. Rotor currents Ir_{abc} of DPC-NSTSMC.

respectively. So the proposed strategy has the least change, as this change was estimated at percentages of 17.69 % and 16.16 % for both the traditional and proposed strategy, respectively. Therefore, the proposed strategy is highly efficient and robust compared to the traditional strategy.

In Tables 5 and 6, a comparison is made between the proposed control and some works in terms of response time and THD of current. These two tables give a clear picture of the superiority of the proposed strategy over some existing controls in terms of reducing the response time of power and

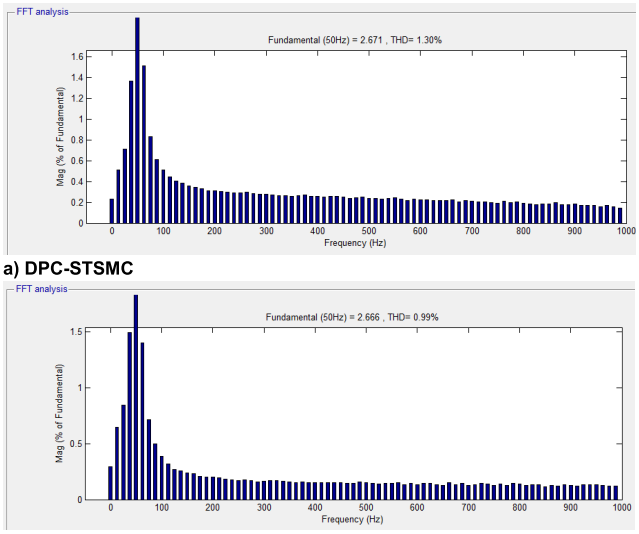

FIGURE 36. THD of Is_a currents.

TABLE 4. The THD value changed in the two tests.

	THD value of current	
	DPC-STSMC	DPC-NSTSMC-SVPWM
Test_1	1.07 %	0.83 %
Test_2	1.30 %	0.99 %
The difference	+ 0.23 %	+ 0.16 %
Ratios	17.69 %	16.16 %

TABLE 5. Comparison in terms of response time.

References		Respones Time (ms)	
		Ps (W)	*Qs* (VAR)
[81]	DPC	17 ms	18 ms
	Nonlinear DPC method	9 ms	5 ms
[50]		33.8 ms	34.5 ms
[82]		15 ms	80 ms
[83]		-	28 ms
[61]	Test_1	1.70 ms	1.85 ms
	Test_2	1.34 ms	1.183 ms
DPC-NSTSMC-SVPWM	Test_1	0.011 ms	0.89 ms
	Test_2	0.016 ms	1.2 ms

THD of current. Therefore, the proposed strategy has a satisfactory dynamic response and high current quality compared to several strategies, which is desirable.

IV. IMPLEMENTATION RESULTS OF THE PROPOSED STRATEGY

The suggested command is implemented on the dSPACEDS1104 R&D controller Board on a computer running the MATLAB (R2021a) program to carry out and execute the designed command. According to Figure 37, the controller board transmits the required signals to the inverter's IGBTs. This diagram illustrates how dSPACE interacts with a WEG system built on DFIG.

TABLE 6. Comparison in terms of THD value.

Techniques	THD (%)	References
DPC-HOSMC	1.66	[84]
Virtual flux DPC	4.88	[85]
DPC with neuro-fuzzy algorithm	2.72	[86]
Intelligent DTC	4.80	[35]
SOSMC	3.13	[73]
FOC	3.70	[3]
ISMC	0.88	[86]
Multi-resonant-based SMC	3.2	[87]
Predictive DTC	2.15	[88]
Test_1	0.83	DPC-NSTSMC-SVPWM
Test_2	0.99	

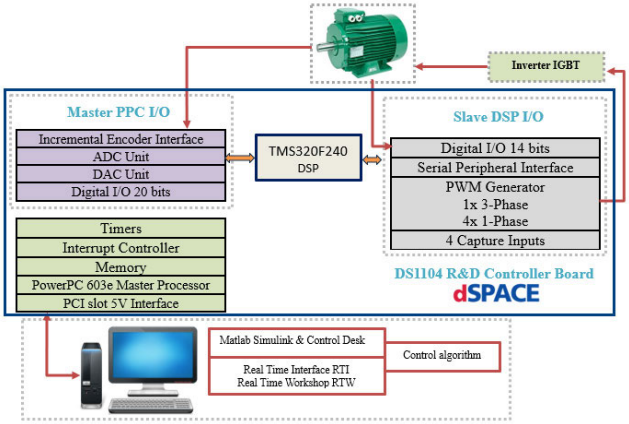

FIGURE 37. Hardware-in-the-Loop (HIL) Diagram of the implemented system.

Four crucial phases are involved in the implementation of the suggested NSTSMC control system in the dSPACE DS1104 hardware:

- **Phase1**: in the MATLAB environment, development and design of the control system model.
- **Phase 2**: C code generation using of the control system using a real-time interface (RTI).
- **Phase 3**: Upload the generated C code into the DS1104 Controller by the Control Desk software.
- **Phase 4:** Run and execute the control system in real time and visualize the results through the Control Desk interface.

The DS1104 R&D Controller Board upgrades a personal computer (PC) to a development system for rapid command prototyping. The board can be installed in virtually any PC with a 5 V free PCI or PCIe slot. It is a cost-effective system with a real-time processor (Figure 38). The combination of MATLAB software with the dSPACE controller gives an efficient, high, and powerful development environment. The function models can be easily run on the DS1104 R&D controller board with its Real-Time Interface (RTI). All Inputs/Outputs (I/O) can be, easily, and graphically configured. All command system blocks will be added to a Simulink block diagram, and Simulink®Coder TM builds

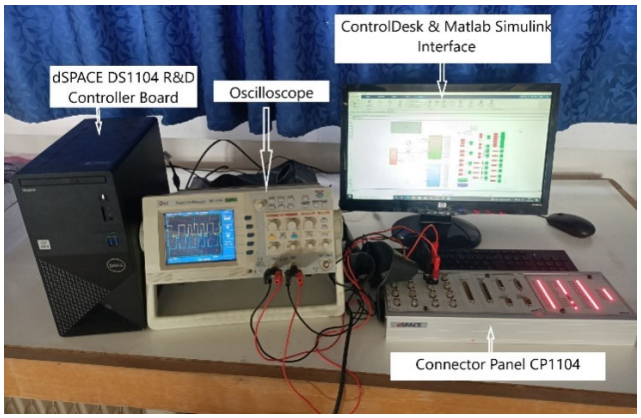

FIGURE 38. Test bench of the HIL setups of the designed control system and WECS.

FIGURE 39. Wind speed profile.

the model code. Using RTI, the model code will be generated via Simulink®Coder™(formerly Real-Time Workshop). The Control Desk software can be used to configure the Outputs/Inputs of the command system graphically. The real-time (rt Model) model will be compiled, downloaded, and started automatically. This fact reduces the implementation time to a minimum. The real-time (rt Model) model will be compiled, downloaded, and started automatically. This fact reduces development costs and the implementation time to a minimum. In addition, it increases the performance and the productivity [61].

The DS1104 controller board collects from the WECS all measurements requested by the designed strategy using and the real-time workshop (RTW) tool and the real-time interface (RTI). The dSPACE DS1104 controller is well-used for controlling the system. The Secondary DSP, Texas Instruments TMS320F240 DSP, generates PWM signals and the PowerPC (PPC 603e core) calculates the simulated controller model. The PWM signals are extracted from the secondary Inputs/Outputs PWM connector on the connection panel CP1104 connector panel and it is visualized on the digital oscilloscope (see Figure 38) [61]. with the use of the Dspace R&D controller the real-time workshop tool, experimental

FIGURE 40. Mechanical power.

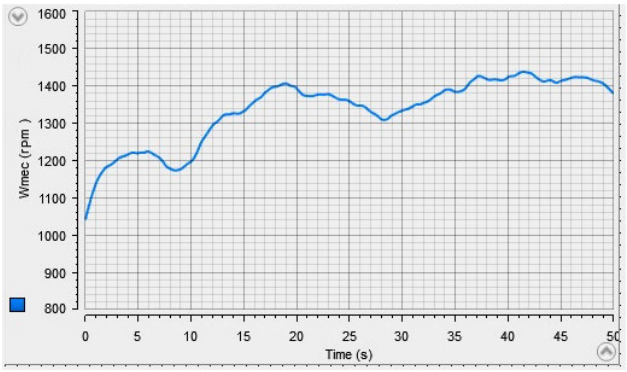

FIGURE 41. Mechanical angular speed.

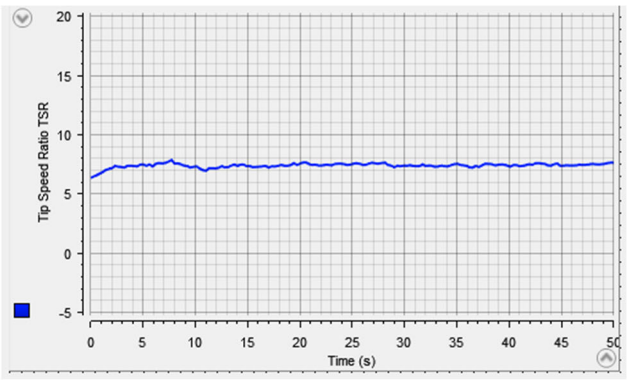

FIGURE 42. Tip speed ratio TSR.

validation, and tests were conducted as part of the suggested method (see Figures 37 and 38).

This work demonstrates that, in contrast to other tactics, this strategy is simple, affordable, and does not require specialists or a sophisticated program. As a result, the proposed command can be applied more broadly in the future. The following figures display the outcomes of our experimental investigation. Utilizing a fluctuating wind profile, this test is designed to demonstrate the tracking effectiveness and regulation of the suggested command. The primary conclusion that can be concluded from these experimental real-time

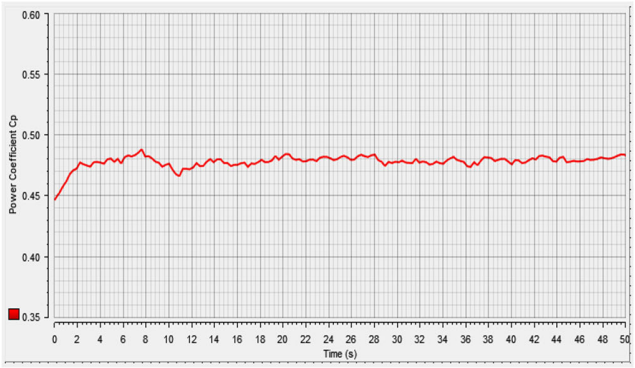

FIGURE 43. Power coefficient Cp.

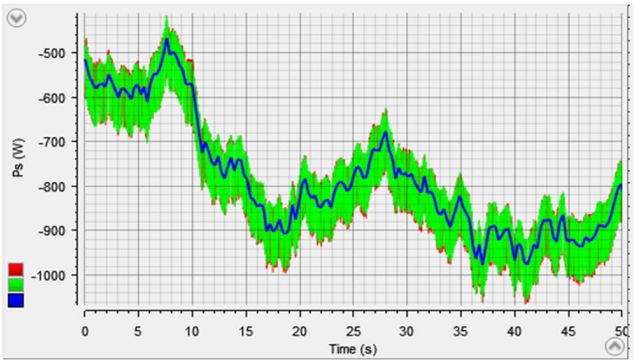

FIGURE 44. Active power Ps.

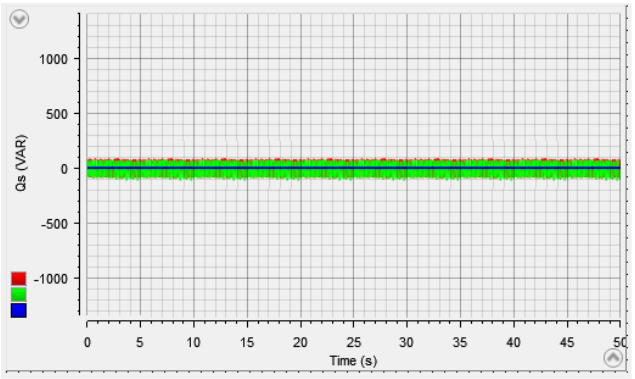

FIGURE 45. Reactive power Qs.

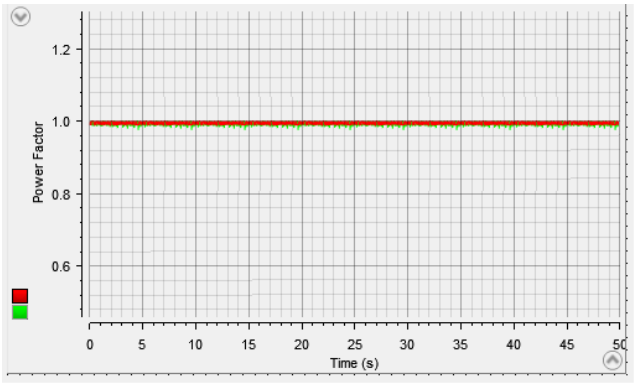

FIGURE 46. Power factor PF.

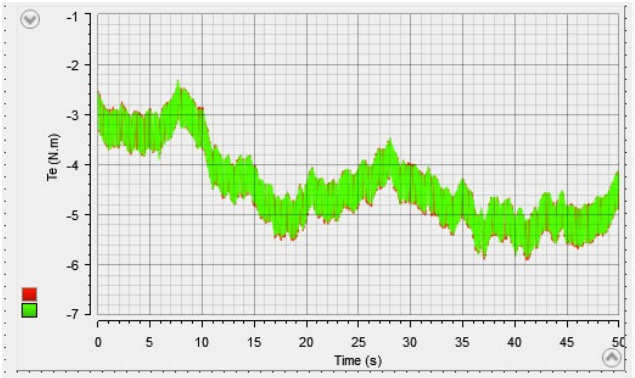

FIGURE 47. Electromagnetic torque Te.

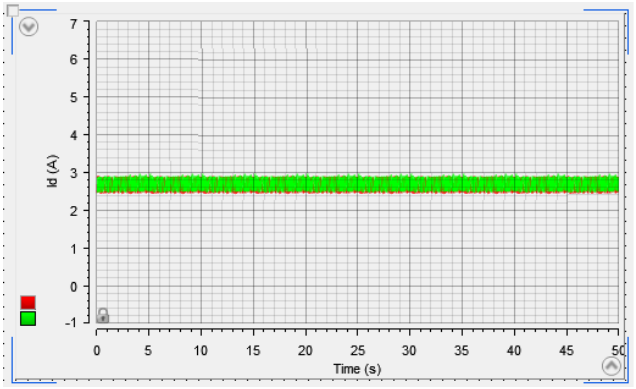

FIGURE 48. Direct rotor current I_{dr}.

results findings is that they are consistent with the conclusions reached through the numerical simulation. Nearly the same behavior was found in both the experimental investigation and the numerical study.

Experimental results are represented in Figures 39-51. It is noted that the experimental validation real-time results confirm the results obtained by the MATLAB 2021a simulations. Figures 39 and 40 represent both the WS and the mechanical power gained from the wind. It is noted that the power gained from the wind takes the form of a change in the WS, which is the same as the turbine's rotational speed represented in Figure 41. The rotation speed changes according to the change in the wind's real speed. The system speed increases with the increase in real WS profile and decreases with its decrease. Figure 42 represents the TSR, which is almost the same as that obtained in the simulation, as it takes a constant value of approximately 7.20. Figure 43 represents Cp. The latter takes a value of approximately 0.48 with ripples, as it does not change with the change of WS.

The supplied system power *Ps* and *Qs* are represented in Figures 44 and 45, respectively. These figures show that the change in the *Ps* is associated with a significant change in WS with the presence of fluctuations and ripples, as these ripples

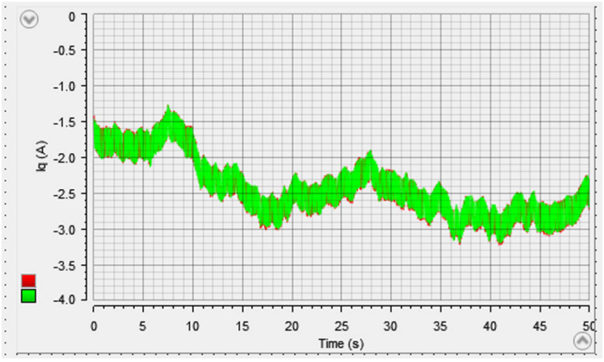

FIGURE 49. Quadrature rotor current I_{qr}.

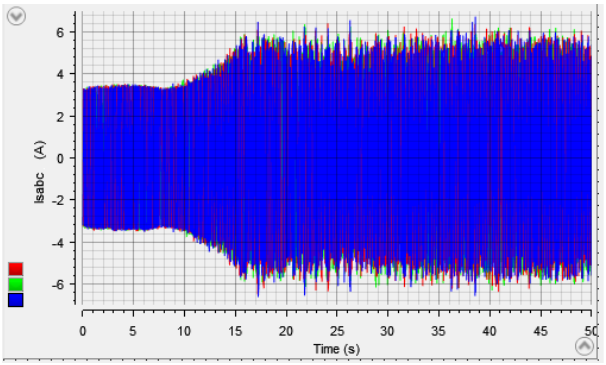

a)DPC-STSMC

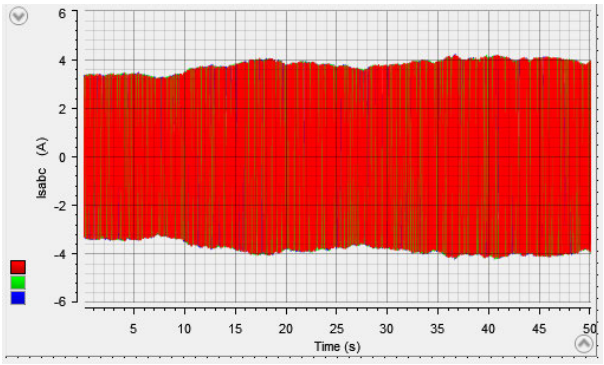

b) DPC-NSTSMC

FIGURE 50. Stator currents (Is_{abc}).

are greater in the case of using DPC-STSMC technique compared to the DPC-NSTSMC technique. Also, ripples are observed at the level of *Qs* in Figure 45. The latter is less in the case of using DPC-NSTSMC-SVPWM technique compared to the DPC-STSMC technique and it is the same as the results obtained in the simulation. Figure 46 represents energy factor. This latter is equal to the value of 1 in the case of the DPC-NSTSMC-SVPWM with larger ripples in the DPC-STSMC technique compared to the DPC-NSTSMC-SVPWM technique. Figure 47 represents the torque, as this torque takes the Ps change with the presence of ripples. These fluctuations are larger in the DPC-STSMC technique case than the DPC-NSTSMC-SVPWM technique, which is the same as the simulation results.

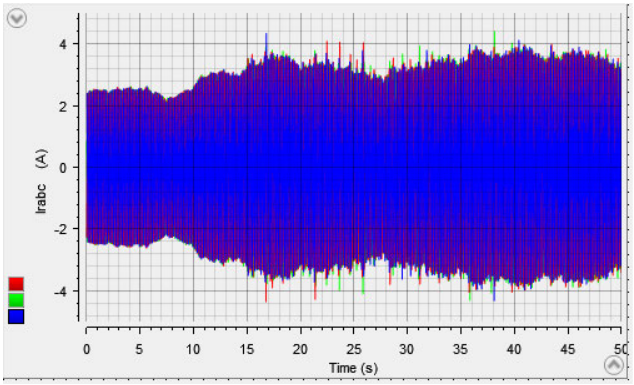

a)DPC-STSMC

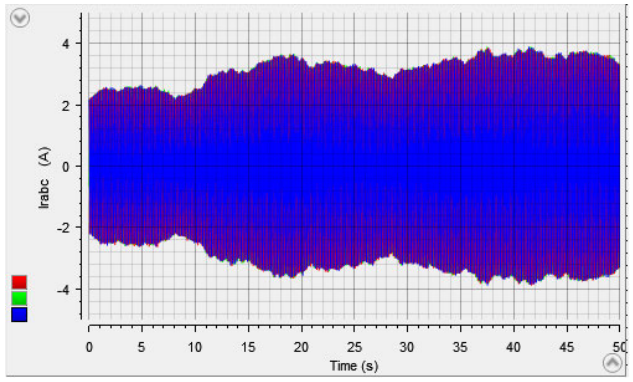

b) DPC-NSTSMC-SVPWM

FIGURE 51. Rotor currents (Ir_{abc}).

Figures 48 and 49 represent the quadrature rotor currents and direct rotor currents of DFIG, respectively. Ripples are observed in the direct rotor current, whose value is not affected by the change in *Ps*. These ripples are larger in the case of DPC-STSMC technique compared to the DPC-NSTSMC-SVPWM technique. For quadrature rotor current, its value is related to the change in wind speed profile, as ripples are observed. The latter is greater when using DPC-STSMC technique compared to the DPC-NSTSMC-SVPWM technique. Also, stator and rotor currents are represented in Figures 50 and 51. These currents are significantly related to the change of *Ps* and WS and are the same as the simulation results.

V. CONCLUSION

This work presents a method for implementing an intelligent super-twisting sliding mode control on the dSPACE card. Neural networks are proposed as the best solution in this work to enhance the nonlinear strategy used to control DFIG power because of their high accuracy, resilience, and robustness. In the designed command, the sign(u) has been replaced by an ANN. The simulated and experimental results showed that the suggested command (neural super-twisting sliding mode control) performs better than the conventional command in terms of reference tracking, minimizing energy ripples, and improving current quality.

In the future, other experimental works will be launched using modern techniques based on the combination of commands, such as the combination of synergetic command and backstepping command, to obtain strong control that greatly facilitates the characteristics of the power generation system.

REFERENCES

[1] H. Benbouhenni, N. Bizon, I. Colak, M. I. Mosaad, and M. Yessef, "Direct active and reactive powers control of double-powered asynchronous generators in multi-rotor wind power systems using modified synergetic control," *Energy Rep.*, vol. 10, pp. 4286–4301, Nov. 2023, doi: 10.1016/j.egyr.2023.10.085.

[2] S. Kadi, H. Benbouhenni, E. Abdelkarim, K. Imarazene, and E. M. Berkouk, "Implementation of third-order sliding mode for power control and maximum power point tracking in DFIG-based wind energy systems," *Energy Rep.*, vol. 10, pp. 3561–3579, Nov. 2023, doi: 10.1016/j.egyr.2023.09.187.

[3] F. Amrane, A. Chaiba, B. E. Babes, and S. Mekhilef, "Design and implementation of high performance field oriented control for grid-connected doubly fed induction generator via hysteresis rotor current controller," *Rev. Roum. Sci. Techn.-Electrotechn. Energy*, vol. 61, no. 4, pp. 319–324, 2016.

[4] H. Benbouhenni, H. Gasmi, and I. Colak, "Backstepping control for multi-rotor wind power systems," *Majlesi J. Energy Manage.*, vol. 11, no. 4, pp. 8–15, 2022. [Online]. Available: https://em.majlesi.info/index.php/em/article/view/493

[5] H. Benbouhenni, I. Colak, N. Bizon, A. G. Mazare, and P. Thounthong, "Direct vector control using feedback PI controllers of a DPAG supplied by a two-level PWM inverter for a multi-rotor wind turbine system," *Arabian J. Sci. Eng.*, vol. 48, no. 11, pp. 15177–15193, Nov. 2023, doi: 10.1007/s13369-023-08035-w.

[6] B. Habib, Z. Boudjema, and A. Belaidi, "DFIG-based wind turbine system using four-level FSVM strategy," *Majlesi J. Energy Manage.*, vol. 6, no. 3, pp. 7–19, 2017.

[7] B. Habib, Z. Boudjema, and A. Belaidi, "Neuro-second order sliding mode control of a DFIG supplied by a two-level NSVM inverter for wind turbine system," *Iranian J. Electr. Electron. Eng.*, vol. 14, no. 4, pp. 362–373, 2018.

[8] H. Chojaa, A. Derouich, S. E. Chehaidia, M. Taoussi, O. Zamzoum, M. I. Mosaad, H. Benbouhenni, and M. Yessef, "Advanced control techniques for doubly-fed induction generators based wind energy conversion systems," in *Proc. Global Energy Conf. (GEC)*, Oct. 2022, pp. 282–287, doi: 10.1109/GEC55014.2022.9987088.

[9] H. Benbouhenni, "Comparative study between NSVM and FSVM strategy for a DFIG-based wind turbine system controlled by neuro-second order sliding mode," *Majlesi J. Mech. Syst.*, vol. 7, no. 1, pp. 33–43, 2018.

[10] M. Yessef, B. Bossoufi, M. Taoussi, A. Lagrioui, and H. Chojaa, "Improved hybrid control strategy of the doubly-fed induction generator under a real wind profile," in *Proc. Int. Conf. Digit. Technol. Appl. (ICDTA)*, vol. 211, pp. 1279–1290, 2021, doi: 10.1007/978-3-030-73882-2_117.

[11] Y. Belkhier, R. N. Shaw, M. Bures, M. R. Islam, M. Bajaj, F. Albalawi, A. Alqurashi, and S. S. M. Ghoneim, "Robust interconnection and damping assignment energy-based control for a permanent magnet synchronous motor using high order sliding mode approach and nonlinear observer," *Energy Rep.*, vol. 8, pp. 1731–1740, Nov. 2022, doi: 10.1016/j.egyr.2021.12.075.

[12] H. Chojaa, A. Derouich, O. Zamzoum, S. Mahfoud, M. Taoussi, H. Albalawi, H. Benbouhenni, and M. I. Mosaad, "A novel DPC approach for DFIG-based variable speed wind power systems using DSpace," *IEEE Access*, vol. 11, pp. 9493–9510, 2023, doi: 10.1109/ACCESS.2023.3237511.

[13] B. Habib, "High order sliding mode direct power control of a DFIG supplied by a five-level NSVPWM strategy for the wind energy conversion system," *Tecnica Italiana-Italian J. Eng. Sci.*, vol. 65, no. 1, 2021.

[14] H. Benbouhenni, "ANFIS-sliding mode control of a DFIG supplied by a two-level SVPWM technique for wind energy conversion system," *Int. J. Appl. Power Eng.*, vol. 9, no. 1, pp. 36–47, Apr. 2020.

[15] H. Benbouhenni, "Application of DPC and DPC-GA to the dual-rotor wind turbine system with DFIG," *IAES Int. J. Robot. Autom.*, vol. 10, no. 3, pp. 224–234, Sep. 2021, doi: 10.11591/ijra.v10i3.pp224-234.

[16] B. Habib, "24-sectors DPC-FNN method of DFIG integrated to dual-rotor wind turbine," *Int. J. Appl. Power Eng.*, vol. 10, no. 4, pp. 291–306, 2021.

[17] H. Benbouhenni, "Amelioration effectiveness of torque and rotor flux control applied to the asynchronous generator (AG) for dual-rotor wind turbine using neural third-order sliding mode approaches," *Int. J. Eng., Trans. C, Aspects*, vol. 35, no. 3, pp. 517–530, 2022.

[18] H. Benbouhenni, N. Bizon, I. Colak, P. Thounthong, and N. Takorabet, "Application of fractional-order PI controllers and neuro-fuzzy PWM technique to multi-rotor wind turbine systems," *Electronics*, vol. 11, no. 9, p. 1340, Apr. 2022, doi: 10.3390/electronics11091340.

[19] B. Habib, H. Gasmi, and N. Bizon, "Direct reactive and active power regulation of DFIG using an intelligent modified sliding-mode control approach," *Int. J. Smart Grid-ijSmartGrid*, vol. 6, no. 4, pp. 157–172, 2022, doi: 10.20508/ijsmartgrid.v6i4.266.g252.

[20] M. Taoussi, M. Karim, B Bossoufi, D. Hammoumi, and A. Lagrioui, "Speed backstepping control of the double-fed induction machine drive," *J. Theor. Appl. Inf. Technol.*, vol. 74, no. 2, pp. 189–199, 2015.

[21] M. Yamamoto and O. Motoyoshi, "Active and reactive power control for doubly-fed wound rotor induction generator," *IEEE Trans. Power Electron.*, vol. 6, no. 4, pp. 624–629, Oct. 1991, doi: 10.1109/63.97761.

[22] H. Benbouhenni, "Stator active and reactive power ripples minimization for DVC control of DFIG by using five-level neural space vector modulation," *Acta Electrotechnica Et Inf.*, vol. 19, no. 2, pp. 16–23, 2019.

[23] K.-J. Du, X.-P. Ma, Z.-X. Zheng, C.-S. Li, W.-X. Hu, and K.-S. Dong, "LVRT capability improvement of DFIG-based wind turbines with a modified bridge-resistive-type SFCL," *IEEE Trans. Appl. Supercond.*, vol. 31, no. 8, pp. 1–5, Nov. 2021, doi: 10.1109/TASC.2021.3091114.

[24] X.-Y. Xiao, R.-H. Yang, Z.-X. Zheng, and Y. Wang, "Cooperative rotor-side SMES and transient control for improving the LVRT capability of grid-connected DFIG-based wind farm," *IEEE Trans. Appl. Supercond.*, vol. 29, no. 2, pp. 1–5, Mar. 2019, doi: 10.1109/TASC.2018.2881315.

[25] H. Zhou, P. Ju, Y. Xue, and J. Zhu, "Probabilistic equivalent model of DFIG-based wind farms and its application in stability analysis," *J. Mod. Power Syst. Clean Energy*, vol. 4, no. 2, pp. 248–255, Apr. 2016, doi: 10.1007/s40565-015-0156-5.

[26] Z.-X. Zheng, C.-J. Huang, R.-H. Yang, X.-Y. Xiao, and C.-S. Li, "A low voltage ride through scheme for DFIG-based wind farm with SFCL and RSC control," *IEEE Trans. Appl. Supercond.*, vol. 29, no. 2, pp. 1–5, Mar. 2019, doi: 10.1109/TASC.2019.2891687.

[27] S. Kadi, K. Imarazene, E. M. Berkouk, H. Benbouhenni, and E. Abdelkarim, "A direct vector control based on modified SMC theory to control the double-powered induction generator-based variable-speed contra-rotating wind turbine systems," *Energy Rep.*, vol. 8, pp. 15057–15066, Nov. 2022, doi: 10.1016/j.egyr.2022.11.052.

[28] H. Benbouhenni and N. Bizon, "Advanced direct vector control method for optimizing the operation of a double-powered induction generator-based dual-rotor wind turbine system," *Mathematics*, vol. 9, no. 19, p. 2403, Sep. 2021, doi: 10.3390/math9192403.

[29] H. Benbouhenni, "Comparison study between seven-level SVPWM and two-level SVPWM strategy in direct vector control of a DFIG-based wind energy conversion systems," *Int. J. Appl. Power Eng.*, vol. 9, no. 1, pp. 12–21, Apr. 2020.

[30] B. Habib, "Intelligence indirect vector control of a DFIG based wind turbines," *Majlesi J. Elect. Eng.*, vol. 13, no. 3, pp. 27–35, 2019.

[31] B. Habib, "Comparative study between different vector control methods applied to DFIG wind turbines," *Majlesi J. Mech. Syst.*, vol. 7, no. 4, pp. 15–23, 2018.

[32] H. Benbouhenni, Z. Boudjema, and A. Belaidi, "Indirect vector control of a DFIG supplied by a two-level FSVM inverter for wind turbine system," *Majlesi J. Electr. Eng.*, vol. 13, no. 1, pp. 45–54, 2019.

[33] B. Habib, Z. Boudjema, and A. Belaidi, "Direct vector control of a DFIG supplied by an intelligent SVM inverter for wind turbine system," *Iranian J. Electr. Electron. Eng.*, vol. 15, no. 1, pp. 45–55, 2019.

[34] H. Benbouhenni, Z. Boudjema, and A. Belaidi, "Using three-level Fuzzy space vector modulation method to improve indirect vector control strategy of a DFIG based wind energy conversion systems," *Int. J. Smart Grid*, vol. 2, no. 3, pp. 155–171, 2018.

[35] S. Mahfoud, A. Derouich, N. El Ouanjli, M. El Mahfoud, and M. Taoussi, "A new strategy-based PID controller optimized by genetic algorithm for DTC of the doubly fed induction motor," *Systems*, vol. 9, no. 2, p. 37, May 2021, doi: 10.3390/systems9020037.

[36] H. Benbouhenni, Z. Boudjema, and A. Belaidi, "A comparative study between four-level NSVM and three-level NSVM technique for a DFIG-based WECSs controlled by indirect vector control," *Carpathian J. Electron. Comput. Eng.*, vol. 11, no. 2, pp. 13–19, Dec. 2018.

[37] Z. Boudjema, R. Taleb, Y. Djeriri, and A. Yahdou, "A novel direct torque control using second order continuous sliding mode of a doubly fed induction generator for a wind energy conversion system," *TURKISH J. Electr. Eng. Comput. Sci.*, vol. 25, no. 2, pp. 965–975, 2017, doi: 10.3906/elk-1510-89.

[38] B. Bossoufi, M. Karim, M. Taoussi, H. A. Aroussi, M. Bouderbala, O. Deblecker, S. Motahhir, A. Nayyar, and M. A. Alzain, "Rooted tree optimization for the backstepping power control of a doubly fed induction generator wind turbine: DSPACE implementation," *IEEE Access*, vol. 9, pp. 26512–26522, 2021, doi: 10.1109/ACCESS.2021.3057123.

[39] T. Pham-Dinh, H. Nguyen-Thanh, K. Uchida, and T. N. G. Minh, "Comparison between modifications of SFOC and DPC in control of grid-connected doubly fed induction generator under unbalanced voltage dip," in *Proc. SICE Annu. Conf.*, Nagoya, Japan, Sep. 2013, pp. 2581–2588.

[40] E. Heydari, M. Rafiee, and M. Pichan, "Fuzzy-genetic algorithm-based direct power control strategy for DFIG," *Iranian J. Electr. Electron. Eng.*, vol. 14, no. 4, pp. 353–361, 2018.

[41] H. Benbouhenni, "Direct power control of a DFIG fed by a seven-level inverter using SVM strategy," *Int. J. Smart Grid*, vol. 3, no. 2, pp. 54–62, 2019.

[42] J. G. Norniella, J. M. Cano, G. A. Orcajo, C. H. Rojas, J. F. Pedrayes, M. F. Cabanas, and M. G. Melero, "Improving the dynamics of virtual-flux-based control of three-phase active rectifiers," *IEEE Trans. Ind. Electron.*, vol. 61, no. 1, pp. 177–187, Jan. 2014, doi: 10.1109/TIE.2013.2245614.

[43] H. Salime, B. Bossoufi, S. Motahhir, and Y. El Mourabit, "A novel combined FFOC-DPC control for wind turbine based on the permanent magnet synchronous generator," *Energy Rep.*, vol. 9, pp. 3204–3221, Dec. 2023, doi: 10.1016/j.egyr.2023.02.012.

[44] A. Mehdi, A. Reama, H. E. Medouce, S. E. Rezgui, and H. Benalla, "Direct active and reactive power control of DFIG based wind energy conversion system," in *Proc. Int. Symp. Power Electron., Electr. Drives, Autom. Motion*, Ischia, Italy, Jun. 2014, pp. 1128–1133, doi: 10.1109/SPEEDAM.2014.6872091.

[45] H. Benbouhenni, "Twelve sectors DPC control based on neural hysteresis comparators of the DFIG integrated to wind power," *Tecnica Italiana-Italian J. Eng. Sci.*, vol. 64, nos. 2–4, pp. 347–353, Jun. 2020.

[46] H. Benbouhenni and N. Bizon, "A new direct power control method of the DFIG-DRWT system using neural PI controllers and four-level neural modified SVM technique," *J. Appl. Res. Technol.*, vol. 21, no. 1, pp. 36–55, Feb. 2023.

[47] H. Benbouhenni, Z. Boudjema, and A. Belaidi, "Power control of DFIG in WECS using DPC and NDPC-NPWM methods," *Math. Model. Eng. Problems*, vol. 7, no. 2, pp. 223–236, Jun. 2020.

[48] B. Majout, B. Bossoufi, M. Karim, N. El Ouanjli, I. Saady, Z. E. Z. Laggoun, M. El Mahfoud, and M. Yessef, "Model reference adaptive system based DPC-SVM control for permanent magnet synchronous generator," in *Proc. Digit. Technol. Appl. (ICDTA)*, vol. 454, 2022, pp. 535–544, doi: 10.1007/978-3-031-01942-5_53.

[49] L. Shang and J. Hu, "Sliding-mode-based direct power control of grid-connected wind-turbine-driven doubly fed induction generators under unbalanced grid voltage conditions," *IEEE Trans. Energy Convers.*, vol. 27, no. 2, pp. 362–373, Jun. 2012, doi: 10.1109/TEC.2011.2180389.

[50] P. Xiong and D. Sun, "Backstepping-based DPC strategy of a wind turbine-driven DFIG under normal and harmonic grid voltage," *IEEE Trans. Power Electron.*, vol. 31, no. 6, pp. 4216–4225, Jun. 2016, doi: 10.1109/TPEL.2015.2477442.

[51] H. Benbouhenni and N. Bizon, "Terminal synergetic control for direct active and reactive powers in asynchronous generator-based dual-rotor wind power systems," *Electronics*, vol. 10, no. 16, p. 1880, Aug. 2021, doi: 10.3390/electronics10161880.

[52] B. Habib, "Direct active and reactive powers command with third-order sliding mode theory for DFIG-based dual-rotor wind power systems," *Int. J. Natural Eng. Sci.*, vol. 15, no. 1, pp. 17–34, 2021.

[53] H. Benbouhenni, F. Mehedi, and L. Soufiane, "New direct power synergetic-SMC technique based PWM for DFIG integrated to a variable speed dual-rotor wind power," *Automatika*, vol. 63, no. 4, pp. 718–731, Dec. 2022, doi: 10.1080/00051144.2022.2065801.

[54] H. Benbouhenni, D. Zellouma, N. Bizon, and I. Colak, "A new PI(1+PI) controller to mitigate power ripples of a variable-speed dual-rotor wind power system using direct power control," *Energy Rep.*, vol. 10, pp. 3580–3598, Nov. 2023, doi: 10.1016/j.egyr.2023.10.007.

[55] H. Benbouhenni, E. Bounadja, H. Gasmi, N. Bizon, and I. Colak, "A new PD(1+PI) direct power controller for the variable-speed multi-rotor wind power system driven doubly-fed asynchronous generator," *Energy Rep.*, vol. 8, pp. 15584–15594, Nov. 2022, doi: 10.1016/j.egyr.2022.11.136.

[56] H. Benbouhenni, I. Colak, and N. Bizon, "Application of genetic algorithm and terminal sliding surface to improve the effectiveness of the proportional–integral controller for the direct power control of the induction generator power system," *Eng. Appl. Artif. Intell.*, vol. 125, Oct. 2023, Art. no. 106681, doi: 10.1016/j.engappai.2023.106681.

[57] H. Benbouhenni, H. Gasmi, I. Colak, N. Bizon, and P. Thounthong, "Synergetic-PI controller based on genetic algorithm for DPC-PWM strategy of a multi-rotor wind power system," *Sci. Rep.*, vol. 13, no. 1, Aug. 2023, Art. no. 13570, doi: 10.1038/s41598-023-40870-7.

[58] H. Benbouhenni, M. I. Mosaad, I. Colak, N. Bizon, H. Gasmi, M. Aljohani, and E. Abdelkarim, "Fractional-order synergetic control of the asynchronous generator-based variable-speed multi-rotor wind power systems," *IEEE Access*, vol. 11, pp. 133490–133508, 2023, doi: 10.1109/ACCESS.2023.3335902.

[59] H. Benbouhenni, G. Hamza, M. Oproescu, N. Bizon, P. Thounthong, and I. Colak, "Application of fractional-order synergetic-proportional integral controller based on PSO algorithm to improve the output power of the wind turbine power system," *Sci. Rep.*, vol. 14, no. 1, p. 609, Jan. 2024, doi: 10.1038/s41598-024-51156-x.

[60] H. Benbouhenni, N. Bizon, P. Thounthong, I. Colak, and P. Mungporn, "A new integral-synergetic controller for direct reactive and active powers control of a dual-rotor wind system," *Meas. Control*, vol. 57, no. 2, pp. 208–224, Feb. 2024, doi: 10.1177/00202940231195117.

[61] M. Yessef, H. Benbouhenni, M. Taoussi, A. Lagrioui, I. Colak, B. Bossoufi, and T. A. H. Alghamdi, "Experimental validation of feedback PI controllers for multi-rotor wind energy conversion systems," *IEEE Access*, vol. 12, pp. 7071–7088, 2024, doi: 10.1109/ACCESS.2024.3351355.

[62] H. Benbouhenni, N. Bizon, M. I. Mosaad, I. Colak, A. B. Djilali, and H. Gasmi, "Enhancement of the power quality of DFIG-based dual-rotor wind turbine systems using fractional order fuzzy controller," *Expert Syst. Appl.*, vol. 238, Mar. 2024, Art. no. 121695, doi: 10.1016/j.eswa.2023.121695.

[63] H. Benbouhenni, I. Colak, N. Bizon, and E. Abdelkarim, "Fractional-order neural control of a DFIG supplied by a two-level PWM inverter for dual-rotor wind turbine system," *Meas. Control*, vol. 57, no. 3, pp. 301–318, Mar. 2024.

[64] H. Benbouhenni and S. Lemdani, "Combining synergetic control and super twisting algorithm to reduce the active power undulations of doubly fed induction generator for dual-rotor wind turbine system," *Electr. Eng. Electromechanics*, no. 3, pp. 8–17, Jun. 2021, doi: 10.20998/2074-272x.2021.3.02.

[65] N. Debdouche, L. Zarour, A. Chebabhi, N. Bessous, H. Benbouhenni, and I. Colak, "Genetic algorithm-super-twisting technique for grid-connected PV system associate with filter," *Energy Rep.*, vol. 10, pp. 4231–4252, Nov. 2023, doi: 10.1016/j.egyr.2023.10.074.

[66] H. Gasmi, M. Sofiane, H. Benbouhenni, and N. Bizon, "Optimal operation of doubly-fed induction generator used in a grid-connected wind power system," *Iranian J. Electr. Electron. Eng.*, vol. 19, no. 2, p. 2431, 2023, doi: 10.22068/IJEEE.19.2.2431.

[67] H. Gasmi, H. Benbouhenni, S. Mendaci, and I. Colak, "A new scheme of the fractional-order super twisting algorithm for asynchronous generator-based wind turbine," *Energy Rep.*, vol. 9, pp. 6311–6327, Dec. 2023, doi: 10.1016/j.egyr.2023.05.267.

[68] H. Gasmi, S. Mendaci, S. Laifa, W. Kantas, and H. Benbouhenni, "Fractional-order proportional-integral super twisting sliding mode controller for wind energy conversion system equipped with doubly fed induction generator," *J. Power Electron.*, vol. 22, no. 8, pp. 1357–1373, Aug. 2022, doi: 10.1007/s43236-022-00430-0.

[69] N. Debdouche, B. Deffaf, H. Benbouhenni, Z. Laid, and M. I. Mosaad, "Direct power control for three-level multifunctional voltage source inverter of PV systems using a simplified super-twisting algorithm," *Energies*, vol. 16, no. 10, p. 4103, May 2023, doi: 10.3390/en16104103.

[70] H. Benbouhenni and H. Gasmi, "Comparative study of synergetic controller with super twisting algorithm for rotor side inverter of DFIG," *Int. J. Smart Grid-ijSmartGrid*, vol. 6, no. 4, pp. 144–156, 2022, doi: 10.20508/ijsmartgrid.v6i4.265.g251.

[71] A. Almakki, A. Mazalov, H. Benbouhenni, and N. Bizon, "Comparison of two fractional-order high-order SMC techniques for DFIG-based wind turbines: Theory and simulation results," *ECTI Trans. Electr. Eng., Electron., Commun.*, vol. 21, no. 2, Jun. 2023, Art. no. 249817, doi: 10.37936/ecti-eec.2023212.249817.

[72] H. Benbouhenni, N. Bizon, I. Colak, P. Thounthong, and N. Takorabet, "Simplified super twisting sliding mode approaches of the double-powered induction generator-based multi-rotor wind turbine system," *Sustainability*, vol. 14, no. 9, p. 5014, Apr. 2022, doi: 10.3390/su14095014.

[73] A. Yahdou, B. Hemici, and Z. Boudjema, "Second order sliding mode control of a dual-rotor wind turbine system by employing a matrix converter," *J. Electr. Eng.*, vol. 16, pp. 1–11, Jan. 2016.

[74] B. Habib, "A novel direct active and reactive power control method using fuzzy super twisting algorithms and modified space vector modulation technique for an asynchronous generator-based dual-rotor wind powers," *Iranian J. Energy Environ.*, vol. 12, no. 2, pp. 109–117, 2021.

[75] B. Habib, "Utilization of an ANFIS-STSM algorithm to minimize total harmonic distortion," *Int. J. Smart Grid*, vol. 4, no. 2, pp. 56–67, 2020.

[76] H. Benbouhenni, Z. Boudjema, and A. Belaidi, "DPC based on ANFIS super-twisting sliding mode algorithm of a doubly-fed induction generator for wind energy system," *J. Européen des Systèmes Automatisés*, vol. 53, no. 1, pp. 69–80, Feb. 2020.

[77] H. Benbouhenni, "Second order sliding mode with ANFIS controllers for DFIG using seven-level NSVPWM technique," *Majlesi J. Energy Manage.*, vol. 8, no. 1, pp. 29–39, 2019.

[78] H. Benbouhenni, "A comparative study between NSMC and NSOSMC strategy for a DFIG integrated into wind energy system," *Carpathian J. Electron. Comput. Eng.*, vol. 12, no. 1, pp. 1–8, Sep. 2019.

[79] H. Benbouhenni, "Stator current and rotor flux ripples reduction of DTC DFIG drive using FSTSMC algorithm," *Int. J. Smart Grid*, vol. 3, no. 4, 2019. [Online]. Available: https://www.ijsmartgrid-org.ijrer.org/index.php/ijsmartgridnew/article/view/82

[80] H. Benbouhenni, "Rotor flux and torque ripples minimization for direct torque control of DFIG by NSTSM algorithm," *Majlesi J. Energy Manage.*, vol. 7, no. 3, pp. 1–9, 2018.

[81] Y. Ibrahim, A. Semmah, and W. Patrice, "Neuro-second order sliding mode control of a DFIG based wind turbine system," *J. Electr. Electron. Eng.*, vol. 13, pp. 63–68, Jan. 2020.

[82] H. E. Alami, B. Bossoufi, S. Motahhir, E. H. Alkhammash, M. Masud, M. Karim, M. Taoussi, M. Bouderbala, M. Lamnadi, and M. El Mahfoud, "FPGA in the loop implementation for observer sliding mode control of DFIG-generators for wind turbines," *Electronics*, vol. 11, no. 1, p. 116, Dec. 2021, doi: 10.3390/electronics11010116.

[83] H. Chojaa, A. Derouich, S. E. Chehaidia, O. Zamzoum, M. Taoussi, and H. Elouatouat, "Integral sliding mode control for DFIG based WECS with MPPT based on artificial neural network under a real wind profile," *Energy Rep.*, vol. 7, pp. 4809–4824, Nov. 2021, doi: 10.1016/j.egyr.2021.07.066.

[84] I. Yaichi, A. Semmah, P. Wira, and Y. Djeriri, "Super-twisting sliding mode control of a doubly-fed induction generator based on the SVM strategy," *Periodica Polytechnica Electr. Eng. Comput. Sci.*, vol. 63, no. 3, pp. 178–190, Jun. 2019, doi: 10.3311/ppee.13726.

[85] N. A. Yusoff, A. M. Razali, K. A. Karim, T. Sutikno, and A. Jidin, "A concept of virtual-flux direct power control of three-phase AC–DC converter," *Int. J. Power Electron. Drive Syst.*, vol. 8, no. 4, pp. 1776–1784, 2017, doi: 10.11591/ijpeds.v8i4.pp1776-1784.

[86] Y. Sahri, S. Tamalouzt, F. Hamoudi, S. L. Belaid, M. Bajaj, M. M. Alharthi, M. S. Alzaidi, and S. S. M. Ghoneim, "New intelligent direct power control of DFIG-based wind conversion system by using machine learning under variations of all operating and compensation modes," *Energy Rep.*, vol. 7, pp. 6394–6412, Nov. 2021, doi: 10.1016/j.egyr.2021.09.075.

[87] Y. Quan, L. Hang, Y. He, and Y. Zhang, "Multi-resonant-based sliding mode control of DFIG-based wind system under unbalanced and harmonic network conditions," *Appl. Sci.*, vol. 9, no. 6, p. 1124, Mar. 2019, doi: 10.3390/app9061124.

[88] M. A. Mossa, H. Echeikh, and A. Iqbal, "Enhanced control technique for a sensor-less wind driven doubly fed induction generator for energy conversion purpose," *Energy Rep.*, vol. 7, pp. 5815–5833, Nov. 2021, doi: 10.1016/j.egyr.2021.08.183.

MOURAD YESSEF was born in Taounate, Morocco. He received the master's degree in sciences and technology entitled microelectronic from the Faculty of Sciences, Sidi Mohamed Ben Abdallah (SMBA) University, Fes, Morocco. He is currently pursuing the joint Ph.D. degree in electrical engineering with the Faculty of Sciences, SMBA University, and the Higher National School of Arts and Trades (ENSAM-Meknes), Moulay Ismail University, Meknes, Morocco. His research interests include renewable energy, smart grids, artificial intelligence, embedded systems, control systems, and power electronics.

HABIB BENBOUHENNI was born in Chlef, Algeria. He received the M.A. degree in automatic and industrial informatics, in 2017, and the Ph.D. degree in electrical engineering from ENPO-MA, Oran, Algeria. He is currently a Professor with Nişantaşi University, Turkey. He is an editor of seven books and more than 200 papers in scientific fields related to electrical engineering. His research interest includes the application of robust control in wind turbine power systems. In recent years, he has served as a Committee Member of several scientific conferences, such as ECAI-2024 and ECA-2023. He is also a Committee Member of *Symmetry* and *EPCS* journals.

MOHAMMED TAOUSSI was born in Fez, Morocco. He received the master's degree in industrial electronics and the Ph.D. degree in electrical engineering from the Faculty of Sciences, Sidi Mohammed Ben Abdellah (SMBA) University, Fes Morocco, in 2013 and 2018, respectively. He is currently a Professor with SMBA University. His research interests include static converters, electrical motor drives, power electronics, smart grids, renewable energy, and artificial intelligence.

AHMED LAGRIOUI received the Ph.D. degree in electrical engineering from the Mohammadia School of Engineers (EMI), Rabat, Morocco, the aggregation degree in electrical engineering from the ENSET School, Rabat, in 2003, and the DESA degree in industrial electronics from EMI. He is currently a Professor with the Higher National School of Arts and Trades (ENSAM-Meknes), Moulay Ismail University, Meknes, Morocco. His research interests include static converters, electrical machines, control systems, and power electronics.

ILHAMI COLAK was born in Turkey, in 1962. He received the Diploma degree in electrical engineering and the M.Sc. degree in electrical engineering in the field of speed control of wound rotor induction machines using semiconductor devices from Gazi University, in 1985 and 1991, respectively, the M.Phil. degree from the University of Birmingham, U.K., in 1991, and the Ph.D. degree from Aston University, U.K., in 1994, with a focus on mixed frequency testing of induction machines using inverters. He became an Assistant Professor, an Associate Professor, and a Full Professor, in 1995, 1999, and 2005, respectively. He has published more than 108 journal articles, 239 conference papers, and seven books on different subjects, including electrical machines, drive systems, machine learning, reactive power compensation, inverters, converters, artificial neural networks, distance learning automation, and alternating energy sources.

SALEH MOBAYEN (Senior Member, IEEE) received the B.Sc. and M.Sc. degrees in control engineering from the University of Tabriz, Tabriz, Iran, in 2007 and 2009, respectively, and the Ph.D. degree in control engineering from Tarbiat Modares University, Tehran, Iran, in January 2013. Since December 2018, he has been an Associate Professor of control engineering with the Department of Electrical Engineering, University of Zanjan. He currently cooperates with the National Yunlin University of Science and Technology. He has published many papers in national and international journals. He serves as a member of the program committee of IEEE conferences.

ANTON ZHILENKOV (Senior Member, IEEE) received the specialist degree in control engineering from Kerch State Maritime Technological University, Kerch, Russia, in 2003, and the Ph.D. degree in control engineering from the Admiral Makarov State University of Maritime and Inland Shipping, Russia, in December 2014. Since December 2018, he has been the Head of the Department of Cyber-physical Systems and the Research Laboratory of Cyber-Physical Systems, Saint Petersburg State Marine Technical University, Russia. He has published many articles in national and international journals.

BADRE BOSSOUFI was born in Fes, Morocco, on 1985. He received the Ph.D. degree in electrical engineering from the Faculty of Sciences, Sidi Mohamed Ben Abdellah (SMBA) University, Morocco, and the joint Ph.D. degree from the Faculty of Electronics and Computer, University of Piteşti, Romania, and the Montefiore Institute of Electrical Engineering, Belgium, in 2012. He is currently a Professor of electrical engineering with the Faculty of Sciences, SMBA University. He has published more than 132 journal and conference papers indexed in Scopus and/or Web of Sciences (WoS). His research interests include static converters, electrical motor drives, power electronics, smart grids, renewable energy, and artificial intelligence. He was named one of the top 2% scientists Worldwide in 2023 by Stanford University.